



TECHNISCHE
UNIVERSITÄT
WIEN
Vienna University of Technology

DIPLOMARBEIT

Development of Microvascular Networks from Outgrowth Endothelial Cells Cocultured with Adipogenically and Osteogenically Differentiated and Undifferentiated Adipose-Derived Stem Cells in Fibrin

Ausgeführt am Ludwig Boltzmann Institut für
Experimentelle und Klinische Traumatologie

unter der Anleitung von Prof. Dr. Heinz Redl und Dr. Wolfgang Holnthoner
als verantwortlich mitwirkendem Betreuer

durch

Karin Hohenegger, BSc.

3532 Rastendorf, Niedergrünbach 10

Statutory Declaration

I declare that I have authored this thesis independently, that I have not used other than the declared sources / resources, and that I have explicitly marked all material which has been quoted either literally or by content from the used sources.

Date

Signature

Table of Contents

LIST OF ABBREVIATIONS.....	IV
1. Abstract (English Version)	1
2. Abstract (German Version).....	3
3. Theoretical Background	5
3.1 Biological Assembly of the Vasculature	6
3.2 Origins of Endothelial Progenitor Cells and Mural Cells.....	7
3.3 Neovascularization and the Molecular Mechanisms behind.....	8
3.4 Different Approaches for Prevascularization	10
3.5 Prevascularization via Cell Coculture Systems	11
3.6 Fibrin as Scaffold.....	12
4. Aim of the Study	14
5. Materials and Methods.....	15
5.1 Outgrowth Endothelial Cell Isolation.....	15
5.2 Outgrowth Endothelial Cell Culture.....	17
5.3 Origin and Culture of Adipose-derived Stem Cells (ASCs)	18
5.4 Characterization of OECs and ASCs by Surface Protein Profiling via Fluorescence Activated Cell Sorting (FACS)	19
5.5 Differentiation into the Adipogenic and Osteogenic Lineage.....	20
5.6 Cell Seeding onto <i>Cytodex</i> TM 1 Cellulose Beads	22
5.7 Inoculation and Coculture of OECs together with Undifferentiated, Adipogenically and Osteogenically Differentiated ASCs in Fibrin.....	25
5.8 Inoculation and Coculture of OECs together with Undifferentiated, Adipogenically and Osteogenically Differentiated ASCs in Ibidi Slides	26
5.9 Immunoblotting.....	27
5.10 Investigation of different OEC:ASC Cculture Ratios and the Tubular Network Formation with and without <i>Cytodex</i> TM 1 Cellulose Beads	29

5.11	Non-Standardized Quantification of Tubules in <i>Ibidi-μ-Slides</i>	29
5.12	Standardized Quantification of Stained Tubules.....	30
5.1	Placenta Decellularization.....	31
6.	Results	33
6.1	Outgrowth Endothelial Cell Isolation.....	33
6.2	Characterization of OECs and ASCs by Surface Protein Profiling via Fluorescence Activated Cell Sorting (FACS)	33
6.3	Differentiation into the Adipogenic and Osteogenic Lineage.....	35
6.4	Coculture of OECs and ASCs in Fibrin	39
6.4.1	Coculture of OECs with Undifferentiated ASCs, Osteogenically and Adipogenically Differentiated ASCs compared to OEC Monoculture in Fibrin	39
6.4.2	Assembly of the Tubular Structures	41
6.4.3	Staining the Tubular Structures against MMP14 and MMP15	42
6.5.1	Investigation of different OEC:ASC Coculture Ratios and the Tubular Network Formation with and without <i>CytodexTM 1</i> Cellulose Beads	44
6.1	Placental Decellularization	48
7.	Discussion and Conclusion	51
7.1	Outgrowth Endothelial Cell Isolation and Characterization of OECs and ASCs by Flow Cytometry	51
7.2	Differentiation into the Adipogenic and Osteogenic Lineage.....	51
7.3	Coculture of OECs and ASCs in Fibrin	52
7.3.1	Coculture of OECs with Undifferentiated ASCs, Osteogenically and Adipogenically Differentiated ASCs compared to OEC Monoculture in Fibrin	52
7.3.2	Assembly of the Tubular Structures	53
8.	Literature.....	57

LIST OF ABBREVIATIONS

%	percent
®	copyright
°C	degrees celsius
µg	microgram
µl	microlitre
µm	micrometre
µM	micromolar
2D	two dimensional
3D	three dimensional
ABAM	antibiotics/antimycotics
ASCs	adipose-derived stem cells
bFGF	basic fibroblast growth factor
BSA	bovine serum albumin
Ca ²⁺	calcium ions
CaCl ₂	calcium chloride
Cat.no.	catalogue number
CD	cluster of differentiation
cm ²	square centimetre
CO ₂	carbon dioxide
Conc _{actual}	actual concentration, which is desired
Conc _{stock}	stock concentration
DAPI	4',6-diamidin-2-phenylindol
DMEM	dulbecco's modified eagles medium
DMSO	dimethyl sulfoxide
DNAse	protease degrading desoxyribonucleic acid
EBM-2	endothelial nasal medium
ECM	extracellular matrix
Ecs	endothelial cells
EDG-1	endothelial differentiation sphingolipid G-protein-coupled receptor-1
EDTA	ethylenediaminetetraacetic acid
EGM-2	endothelial growth medium

ELISA	enzyme-linked immunosorbent assay
EPCs	endothelial progenitor cells
ESC	embryonic stem cell
Eq.#	number of equation
<i>et al.</i>	lat.: et alii, engl.: and others
etc	lat.: et cetera, engl.: and so on
FACS	fluorescence activated cell sorting
FCS	fetal calf serum
FITC	fluorescein isothiocyanate
Flk-1	fetal liver kinase 1
g	gram
GA-1000	gentamicin sulfate amphotericin-B, 1000x stock
H&E	hematoxylin and eosin
H ₂ O	water
HEPES	(4-(2-hydroxyethyl)-1-piperazineethanesulfonic acid
HLA-ABC	MHC class I, A/B/C
	MHC class II cell surface receptor encoded by the human
HLA-DR	leukocyte antigen complex
HUVECs	human umbilical vein endothelial cells
IBMX	3-isobutyl-1-methylxanthine
IgG	immunoglobulin G
IgG-FITC	immunoglobulin G conjugated to fluorescein
IgG-PE	immunoglobulin G conjugated to phosphatidylethanolamine
KCl	potassium chloride
KDR	kinase inserted domain receptor
KH ₂ PO ₄	monopotassium phosphate
KIU	kallikrein-inhibitor-unit
l	litre
LSM	lymphocyte separation medium
M	molar
MCAM	melanoma cell adhesion molecule
mg	milligram
Mg ²⁺	magnesium ions

MgSO ₄	magnesium sulfate
MHC	major histocompatibility complex
ml	millilitre
mm	millimetre
mM	millimolar
MMP14/MT1-MMP	membrane type 1-matrix metalloproteinases
MMP15/ MT2-MMP	membrane type 2-matrix metalloproteinases
MNCs	mononuclear cells
mRNA	messenger ribonucleic acid
Na ₂ HPO ₄	disodium phosphate
NaCl	sodium chloride
nm	nanometre
OECs	outgrowth endothelial cells
p#	number of passage
P/S	penicillin / streptomycin
	phosphate buffered saline solution without calcium (Ca ²⁺) and magnesium ions (Mg ²⁺),
PBS-	containing 138 mM NaCl and 2.7 mM potassium chloride (KCl), pH 7.4
PDGF	platelet derived growth factor
PDGFR β	platelet derived growth factor receptor beta
PE	phosphatidylethanolamine
PECAM-1	platelet endothelial cell adhesion molecule
PFA	paraformaldehyde
pg	picogram
	potentia hydrogenii (negative decadic logarithm of the molar
pH	concentration of dissolved hydronium (H ₃ O ⁺) ions)
PMSF	phenylmethysulfonylfluoride
PSE9	adobe photoshop elements 9
PTPRC	protein tyrosine phosphatase, receptor type C
r3-IGF-1	insulin-like growth factor 1
rhEGF	recombinant human epidermal growth factor
Rh-bFGF (or FGF-2)	recombinant human fibroblast growth factor basic
RNase	protease degrading ribonucleic acid

rpm	rotations per minute
RT	room temperature
S1P1	sphingosine-1-phosphate-1
SMCs	smooth muscle cells
T25	cell culture flask with an area of 25 square centimetres
T75	cell culture flask with an area of 75 square centimetres
TE	trypsin ethylenediaminetetraacetic acid (EDTA)
TGF- β	transforming growth factor-beta
Tie-2	angiopoietin binding receptor
TM	trade mark
Tris base	tris(hydroxymethyl)aminomethane
U	unit
v/v	volume per volume
VE-Cadherin	vascular endothelial cadherin
VEGF	vascular endothelial growth factor
VEGFR2	vascular endothelial growth factor receptor 2
Vol _{actual}	actual volume of final reagent
Vol _{taken}	volume taken from stock solution
w/v	weight per volume
$\alpha 1\beta 1$	integrin alpha1beta1
$\alpha 2\beta 1$	integrin alpha2beta1
$\alpha 5\beta 1$	integrin alpha5beta1
$\alpha 6\beta 1$	integrin alpha6beta1
α -SMA	alpha- smooth muscle actin
$\alpha v\beta 3$	integrin alpha 5beta3

1. ABSTRACT (ENGLISH VERSION)

In this study microvascular networks were generated by coculture of primary outgrowth endothelial cells, isolated from human peripheral blood, on *Cytodex*TM 1 cellulose beads together with either undifferentiated, osteogenically or adipogenically differentiated adipose-derived stem cells in fibrin. OECs in monoculture in fibrin served as negative controls. The networks were characterized via three different parameters, namely the percentage of beads with sprouts, the number of sprouts per bead and the average length of the sprouts. The use of differentiated ASCs was critically reconsidered after it was found that they were capable of further differentiation into the same and also another lineage in monolayer culture. From this observation, it was deduced, that only undifferentiated ASCs were transferred into fibrin, while intact, differentiated ones could either not be detached from the cell culture plate or did not survive due to the mechanical stress, which they were encountered to during detachment and centrifugation.

Therefore, further investigations were focused on the coculture with undifferentiated ASCs which included the comparison of the generated networks with and without *Cytodex*TM 1 cellulose beads as well as different OEC/ASC coculture ratios. While approximately 10^6 OECs/ml were added into fibrin clots without beads, only 10^5 OECs/ml were present in fibrin clots, when they were previously seeded onto beads. To achieve the same cell density, 10 times more beads would have to be added into fibrin, which would have implicated a great loss of space in fibrin that could otherwise be used for tubule formation. Regarding the differences between the different coculture ratios, it was found, that 5:1 resulted in more and higher anastomosed tubules compared to 1:1 and 2:1. The number of tubules at a ratio of 20:1 was comparable to that at 5:1, though the number of OECs was four fold higher. Based on these considerations, it was concluded, that the coculture of OECs without beads together with ASCs at a ratio of 5:1 was the most favorable condition among the investigated ones.

Finally the approach of generating a macroscopic vascular network by use of a decellularized tissue was picked up. Two vessels of a piece of placental tissue were treated by pumping different detergents through for thirteen days at 4°C. On the days 8 and 11, the vessels were rinsed with an enzymatic digestion solution for 24 hours at 37°C. To determine, whether cells were still lining the vessels, haematoxylin and eosin staining was performed on two microtome-cut, in paraffin casted cross sections. In the first one, originating from the treated vessel, no cell nuclei were present any more. The second one was from a non-treated vessel of the same placental tissue piece and showed a continuous lining of cells on its wall. Due to this result, the decellularization was considered successful. Due to limitations in time for this thesis, the cell behavior in the decellularized tissue was not investigated any more.

Generally, it can be concluded, that both cell types, OECs and ASCs can be obtained from adult patients by minimally invasive biopsy. Thus, autologous pre-vascularized tissue can be regenerated *in vitro* and used for clinical treatment of e.g. myocardial infarction or critical limb ischemia [Schächinger *et al.* 2004, Kawamura *et al.* 2005].

2. ABSTRACT (GERMAN VERSION)

In dieser Studie wurden mikrovaskuläre Gefäßnetze durch Kokultur primärer, ausdifferenzierter Endothelzellen (OECs), isoliert aus menschlichem, peripherem Blut, auf *Cytodex*TM 1 Zellulosekügelchen mit entweder undifferenzierten, osteogen oder adipogen differenzierten, aus Fettgewebe gewonnenen Stammzellen (ASCs) in Fibrin generiert. OEC Monokultur in Fibrin diente als Negativkontrolle. Die Netzwerke wurden anhand von drei verschiedenen Parametern charakterisiert, nämlich dem Prozentanteil von Kügelchen, von welchen Gefäße sprießen, die Anzahl der Sprosse pro Kügelchen und die mittlere Länge der Sprosse. Der Gebrauch differenzierter ASCs wurde kritisch überdacht, nachdem sich herausstellte, dass sie zu weiterer Differenzierung in dieselbe, aber auch die andere Nische differenzieren können. Von dieser Beobachtung ausgehend wurde rückgeschlossen, dass nur undifferenzierte ASCs in Fibrin transferiert wurden, während intakte, differenzierte ASCs entweder nicht von der Zellkulturplatte abgelöst werden konnten, oder sie dem mechanischen Stress beim Herunterlösen und der Zentrifugation ausgesetzt waren, nicht überlebten.

Darum wurden weitere Untersuchungen auf die Kokultur mit undifferenzierten ASCs beschränkt. Unter anderem wurde die Qualität der vaskulären Netzwerke mit und ohne *Cytodex*TM 1 Zellulosekügelchen wie auch verschiedene OEC/ASC Kokulturverhältnisse, nämlich 1:1, 2:1, 5:1 und 20:1 evaluiert. Während die Fibrin-Clots ohne Kügelchen ungefähr 10^6 OECs/ml enthielten, wurden ca. 10^5 OECs/ml auf Kügelchen in die Clots transferiert. Um dieselbe Zelldichte zu erreichen, müssten zehn Mal mehr Kügelchen dem Fibrin zugegeben werden. Das würde allerdings einen großen Verlust an Raum im Fibrin mit sich bringen, welcher aber für die Bildung von Gefäßen genutzt werden muss. Hinsichtlich der verschiedenen Zellzahlen, das Kokultur-Verhältnis 5:1 resultierte in mehr und besser verzweigten Gefäßen verglichen mit 1:1 und 2:1. Die Anzahl von Gefäßen bei einem Verhältnis von 20:1 war vergleichbar mit der von 5:1, obwohl die Zahl der OECs vierfach höher war. Aufgrund dieser Betrachtungen wurde beschlossen, dass die Kokultur von OECs ohne Kügelchen mit ASCs im Verhältnis 5:1 die günstigste Variante unter den untersuchten war.

Letztendlich wurde der Ansatz makroskopische, vaskuläre Gefäßnetze aus dezellularisiertem Gewebe zu bilden, aufgegriffen. Ein Stück Plazentagewebe wurde dezellularisiert, indem verschiedene Detergenzien für 13 Tage bei 4°C durch die Gefäße gepumpt wurden. An den Tagen 8 und 11 wurden die Gefäße mit einer enzymatischen Verdauungslösung für 24 Stunden bei 37°C gespült. Um festzustellen, ob die Gefäße danach noch immer mit Zellen ausgekleidet waren, wurde eine Hämatoxylin- und Eosinfärbung von zwei Mikrotom-geschnittenen, in Paraffin gegossenen Querschnitten durchgeführt. Der erste stammte von einem behandelten Gefäß und der zweite von einem nicht-dezellularisierten Gefäß desselben Plazentastückes. Im ersten waren keine Zellkerne mehr präsent, während der zweite Querschnitt eine durchgehende Beschichtung mit Zellen aufwies. Aufgrund dieses Resultats wurde die Dezellularisierung als erfolgreich angesehen. Da die Zeit am Ende dieser Studie schon sehr limitiert war, wurde keine Neubesiedelung des dezellularisierten Plazentagewebes mehr durchgeführt.

Im Allgemeinen kann man zu dem Schluss kommen, dass sowohl OECs als auch ASCs anhand einer minimal invasiven Biopsie von erwachsenen Patienten gewonnen werden können. Deshalb kann autogenetisches, prä-vaskularisiertes Gewebe *in vitro* regeneriert werden und in der Klinik für die Behandlung von z.B. Herzinfarkt oder das Ischämiesyndrom verwendet werden [Schächinger *et al.* 2004, Kawamura *et al.* 2005].

3. THEORETICAL BACKGROUND

Solid tissues and organs of the human body are supplied with nutrients and oxygen by the vascular system, which also removes cellular waste products and carbon dioxide from the sites of production. The vascular system can be divided into the blood vascular system, which comprises the blood vessels and the heart, and the lymphatic vascular system, consisting of lymph vessels and lymph nodes through which the lymph fluid circulates. However, both systems are closely associated during development and are also intimately connected to each other thereafter. The center of the blood vascular system is the heart, which pumps blood through ramifying arteries into the whole body. The large arteries become thinner in diameter and are then called arterioles, which in turn end up into a close-meshed network of microscopic vessels of diameters down to 8 μm , termed capillaries. The membranes of capillaries are composed of single endothelial cells. The capillaries anastomose into venules and finally into veins, which lead back to the heart [Gray, 1918].

Through the network of capillaries, the gas molecules as well as the nutrients diffuse up to distances of 200 μm to the surrounding cells. Sensitive cells like islets only tolerate maximally 100 μm , while cartilage cells are still viable at diffusion distances up to 1 mm [Muschler *et al.*, 2004]. This circumstance needs to be overcome by *in vitro* prevascularization in order to increase the size of tissue and organ grafts. However, prevascularization is not only important for single cell survival but is also essential for fast and successful *in vivo* integration. Since the host's vascularization would be too slow to maintain the graft viable, especially during the first period after implantation, prevascularization is necessary for the survival of the whole implanted constructs. Acquiring knowledge on how to create vascular networks is also of high interest for e.g. treating patients with diabetic eyes, diabetic foot ulcers, cardiovascular or lymphatic diseases.

3.1 Biological Assembly of the Vasculature

Blood vessels in general are composed of distinct cell layers. The intima, the innermost layer, is made up of a single cell type: endothelial cells (EC). The media is composed of layers of mural cells, smooth muscle cells (SMC) in large vessels, and pericytes in microvessels. The outermost layer of large vessels, the adventitia, consists of loose connective tissue containing smaller blood vessels and nerves. In detail, there are three main types of capillaries:

Continuous capillaries: Their inner lining consists of endothelial cells joined together by tight junctions, which allow only small molecules like water or ions to diffuse. There are two types of continuous capillaries which differ in the presence and absence of transport vesicles located between the tight junctions: Those with numerous transport vesicles are primarily found in skeletal muscles, fingers, gonads and skin and the others with few vesicles that are primarily found in the central nervous system. These capillaries are constituents of the blood-brain-barrier.

Fenestrated capillaries: Also their inner lining is built from endothelial cells. However, it appears discontinuous due to pores with diameters from 60 to 80 nm, which are spanned by a diaphragm of radially oriented fibrils. Those pores allow larger molecules like small proteins to diffuse [Pavelka & Roth, 2005]. This type of capillary contains a continuous basal lamina and is found in the endocrine glands, the intestines, the pancreas and the glomeruli of the kidneys.

Sinusoidal capillaries: They are a specific type of fenestrated capillaries that have smaller pores of 30 to 40 μm in diameter in the endothelial cell layer. This vessel type allows red and white blood cells (7.5 and 25 μm , respectively) and proteins to pass. Those capillaries lack pinocytotic vesicles and therefore utilize gaps present in cell junctions to permit transfer between endothelial cells, hence across the membrane. Sinusoid blood vessels are primarily located in the bone marrow, lymph nodes and adrenal gland as well as in the liver and spleen. [Gray. 1918]

3.2 Origins of Endothelial Progenitor Cells and Mural Cells

Endothelial cells or precursors thereof have been found in almost every tissue of the human body. For neovascularization, a fundamental prerequisite is the presence of endothelial progenitor cells (EPCs) in the blood. According to Jain *et al.*, prenatal and postnatal neovascularization fundamentally differ in terms of the endothelial progenitors that build up the vessels. Endothelial cells, which constitute the inner layer of blood vessels, originate from angioblasts in the embryo and in the adult differentiate from endothelial precursor cells that reside quiescent in e.g. the peripheral blood [Amini *et al.*, 2012] and the bone marrow [Asahara *et al.*, 1999; Lin *et al.*, 2000]. However, endothelial cells, characterized by the expression of e.g. kinase inserted domain receptor (KDR), angiopoietin binding receptor (Tie-2), platelet endothelial cell adhesion molecule 1 (PECAM-1) or von Willebrand factor, have been also found abundantly in the spleen and in smaller amounts in the lung, liver, intestine, skin and hind limb muscle as well as in the corpus luteal and endometrium after inductive ovulation [Asahara *et al.*, 1999]. Besides the hypothesis of circulating EPCs, others suggest the existence of a 'vasculogenic zone' in the wall of adult human blood vessels, in which EPCs reside until needed [Zengin *et al.*, 2006], which was to some degree affirmed by the *in vitro* isolation of EPCs from vessel wall derived cultures [Ingram *et al.*, 2005].

Mural cells, which are mainly pericytes and smooth muscle cells, originate from multiple sources during embryonic development, including the local and distal mesenchyme [Hungerford and Little, 1999; Sartore *et al.*, 2001]. In adults, mural cells originate from the bone marrow or its stroma [Carmeliet & Conway, 2001] or via differentiation of fibroblasts into myofibroblasts and finally into vascular smooth muscle cells (SMCs) in response to biochemical or mechanical cues [Chambers *et al.*, 2003; Tomasek *et al.*, 2002; Elenbaas & Weinberg, 2001]. An overview on the cellular origins involved in prenatal and postnatal neovascularization is illustrated in **Figure 1**.

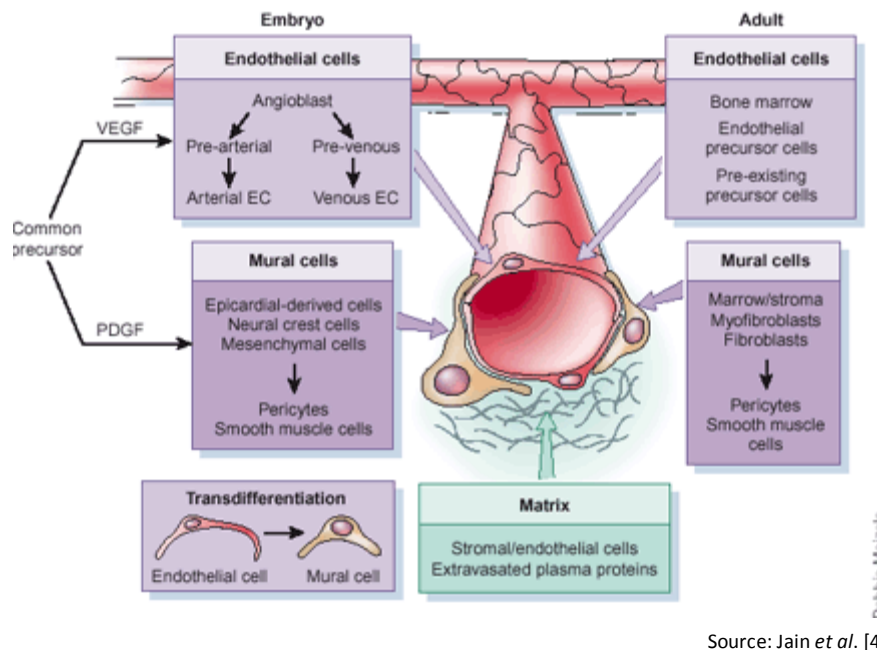


Figure 1: Origin of cells involved in prenatal (left) and postnatal (right) neovascularization.

3.3 Neovascularization and the Molecular Mechanisms behind

The formation of new blood vessels, or neovascularization, comprises two distinct biological processes, namely vasculogenesis – the *de novo* formation of blood vessels and angiogenesis- the sprouting of new blood vessels from already existing ones. Vasculogenesis governs the prenatal formation of the vascular system, giving rise to the very early primitive plexus which matures and remodels and is stabilized by the recruited mural cells [Riseau & Flamme, 1995]. Opinions widely differ concerning postnatal formation of blood vessels. While Kilarski *et al.* states, that wound healing, vascularization of tumors etc. are subjects of angiogenesis, driven by mechanical forces exerted by myofibroblasts, others found high concentrations of EPCs in the centers of subcutaneously implanted, developing tumors as well as in the foci of cutaneous wounds [Kilarski *et al.*, 2009; Asahara *et al.*, 1999]. However, once, the primary vascular vessels are built, they need to be stabilized, which is realized by two mechanisms: on the one hand, recruiting again mural cells and on the other hand, generating extracellular matrix (ECM). This process is regulated by at least four molecular cell signaling pathways which involve: platelet derived growth factor (PDGF) – B-PDGF receptor (PDGFR)- β [Hellström *et al.*, 2001]; sphingosine-1-phosphate-1 (S1P1) – endothelial differentiation sphingolipid G-

protein-coupled receptor-1 (EDG-1) [Kluk & Jöa, 2002]; Angiopoietin 1 – Tie-2 [Yancopoulos et al, 2001; Loughna & Sato, 2001], and transforming growth factor (TGF)- β [Pepper, 1997; Gohongi *et al.*, 1999; Chambers *et al.*, 2003].

De Smet *et al.* reviewed all recent findings and established an even more detailed but nevertheless, leaky hypothesis of the signaling cascades, which might be involved in neovascularization. He stated that those signaling pathways do not occur in each endothelial cell, which participates in tubule formation to the same degree, but rather in three types of specialized cells, which were termed tip, stalk and phalanx cells. The tip cells are the most active ones and located at the forefront of the sprouting vessels. They sense vessel guidance cues through numerous filopodia and lamellipodia, which formation is thought to be mainly induced by Vascular Endothelial Growth Factor (VEGF) [Lamallice *et al.*, 2004]. Before the vessel sprout can be elongated towards proangiogenic stimuli, the surrounding ECM needs to be proteolytically degraded. There is evidence, that this is realized by expression of membrane type 1-matrix metalloproteinases (MT1-MMP or MMP14) by endothelial cells, especially the tip cells [Yana *et al.*, 2007; Davis *et al.*, 2002; van Hinsbergh & Koolwijk, 2008], which might also be regulated by the VEGF receptor-2 (VEGFR2) pathway [Ispanovic *et al.*, 2008]. The stalk cells are less active, which is probably due to lateral inhibition coming from the tip cells [Suchting *et al.*, 2007; Noguera-Troise *et al.*, 2006]. Two mechanisms of vessel lumen formation have been observed in zebrafish embryos: on the one hand, intracellular fusion of ingested vacuoles causes that endothelial cells themselves become elongated; on the other hand, endothelial cells were observed arranging themselves around a lumen, generated by intercellular fusion of ingested vacuoles [Kamei *et al.*, 2006; Blum *et al.*, 2008]. As previously mentioned, primary tubules are stabilized by the formation of new ECM and by the recruitment and association with mural cells. Stalk cells and phalanx cells, which are quiescent endothelial cells, respectively, are stated to be responsible for that according to De Smet. [De Smet *et al.*, 2009].

3.4 Different Approaches for Prevascularization

As previously summarized by Kaully *et al.*, there are generally three different approaches for *in vitro* prevascularization of three-dimensional tissue constructs: coculture of endothelial cells together with target tissue cells and angiogenesis supporting cells; culture of endothelial cells in channels created by microfabrication in engineered tissues; and culture of endothelial cells in decellularized, natural tissues. Another promising approach to enhance tissue vascularization relies on a completely different method, namely direct implantation of polymeric, biodegradable scaffolds with integrated proangiogenic growth factors, like for instance VEGF [Sun *et al.*, 2005; Zhang *et al.*, 2007; Kaigler *et al.*, 2006], basic Fibroblast Growth Factor (bFGF) [Doi *et al.*, 2007; Perets *et al.*, 2003; Hosseinkhani *et al.*, 2006] or a combination of growth factors [Carmeliet, 2000; Richardson *et al.*, 2001; Nillesen *et al.*, 2007], which are constantly released upon *in vivo* degradation mechanisms [Kaully *et al.*, 2009].

Microfabrication of templates on which endothelial cells (ECs) can be cultured is a very 'hands-on' technique, which might be simpler in theory than in practice, since it needs highly sophisticated methods to fabricate networks of sizes in the range of μm . Moreover, it is still unanswered whether endothelial cells, which are cultured on the surface of vessel network templates, show the same expression patterns like endothelial cells, which organize themselves into tubule-like structures upon growth factor signaling and cell-cell contacts as mentioned above. Nevertheless, research has been focused on appropriate fabrication techniques and biodegradable materials. [Leach *et al.*, 2006; Leslie-Barbick *et al.*, 2010; Ceylan *et al.*, 2011; Baudis *et al.*, 2010 and 2011]

Instead of spending huge efforts into mimicking nature, methods have recently been developed focusing on the recycling of natural structures, which means the removal of all cells from the tissue or organ until only the ECM remains. This method is termed 'decellularization' and is achieved by flushing various decellularization agents through the ingoing arteries, arterioles and capillaries as well as the outgoing veins and venules. The striking advantages of this method to those previously described is on the one hand, that the extracellular microenvironment consisting of structural proteins like collagen,

fibronectin and laminin is preserved; on the other hand, the cells are brought into shape immediately after seeding. Ott *et al.* created a whole-heart scaffold with intact geometry and vasculature by decellularizing cadaveric hearts using detergents for coronary perfusion. After decellularization, rat aortic ECs and cardiac cells were reseeded into the vascular system and cocultured at physiological conditions. After 7 days, they formed single layers in larger and smaller coronary vessels, one day thereafter the recellularized heart construct was contracting and responding to drugs [Ott *et al.*, 2008].

3.5 Prevascularization via Cell Coculture Systems

In comparison to the previously described methods for *in vitro* pre-vascularization, coculturing endothelial cells together with angiogenesis mediating cells appears to be the most direct way. Different coculture systems, representing both, pathological as well as physiological vascularization mechanisms have been investigated. Abe *et al.* cocultured bovine aortic endothelial cells and tumor cells of seven glioma cell lines. As a result, stable tubules developed upon coculture of the ECs with those four cell lines, which highly expressed bFGF mRNA while significantly poorer vessel formation occurred during coculture with the other three glioma cell lines expressing bFGF at lower rates [Abe *et al.*, 1993]. In another study, human umbilical vein endothelial cells (HUVECs) were cocultured with either dermal fibroblasts or keratinocytes in a porous chitosan/collagen scaffold in order to reconstruct a cutaneous wound healing model. Vascular network formation was observed in both coculture systems after at least 15 days, while no vascularization occurred in monocultures of each cell type [Black *et al.*, 1999]. However, the most often documented coculture systems include cells which still hold some differentiation potential. For instance, it has been shown in a three dimensional (3D) fibrin matrix that endothelial cells have an improved survival, vascularization and wound healing potential when they are cocultured with cluster of differentiation 34-positive (CD34+), umbilical cord blood- derived stem cells [Pedroso *et al.*, 2011]. Likewise, a vascular system generated by coculture of HUVECs and mesenchymal stem cells in a fibronectin-type I collagen gel was proven to be stable for one year *in vivo* [Koike *et al.*, 2004]. The

differentiation of MSCs into smooth muscle cells was confirmed by Ding *et al.* and Hirschi *et al.*, which further showed that TGF- β and PDGF signaling pathways were involved in its regulation [Ding *et al.*, 2004; Hirschi *et al.*, 1998]. Besides the mediation via growth factors, vascularization also depends on direct cell-cell contacts. Kitahara *et al.* compared the vascular networks build by HUVECs cocultured with mesangial cells in Matrigel®; in one test system cell-cell contact was possible and in the other one, mesangial cells were cultured in an intercup chamber, which physically separated both cell types but allowed sharing the culture medium. In both cases, vascular networks formed, but that of the non-contact system was significantly less developed than that of the contact system [Kitahara *et al.*, 2005]. Opposing to that, barely any capillary-like networks formed in the control system containing HUVECs and growth factor free medium [Nehls *et al.*, 1994].

3.6 Fibrin as Scaffold

As mentioned already several times, vascularization is triggered not only by growth factors and cell-to-cell communication but also by mechanical cues generated by the ECM, which is *in vivo* mainly composed of fibrous, non-globular proteins like collagen, fibrin and laminin. The underlying cellular mechanisms involve interactions between integrins ($\alpha 2\beta 1$, $\alpha 1\beta 1$, $\alpha v\beta 3$, $\alpha 5\beta 1$ and $\alpha 6\beta 1$) and the cytoskeletal macromolecules actin, microtubules and interfilaments. Numerous studies on vessel formation are conducted in Matrigel® [Arnaoutova *et al.*, 2011], a scaffold made from extracellular extracts derived from mouse tumor tissue. Due to its origin and also since it is not well defined, Matrigel® is not suitable for *in vivo* medicinal therapies. Therefore, recent 3D gel assays were performed in gels originating from defined ECM compounds, such as fibrin [Borges *et al.*, 2003; Yang *et al.*, 2012; Barsotti *et al.*, 2011; Kim *et al.*, 2012; Deponti *et al.*, 2012; Man *et al.*, 2011; Nixon *et al.*, 2012], type I collagen [Kanda *et al.*, 2011; Yang *et al.*, 1999; Davis *et al.*, 2002 and 2007; Bayless *et al.*, 2000] or fibronectin [Ribatti *et al.*, 1996]. In this study, fibrin, a physiological, cross linked protein scaffold, the final product in the blood coagulation cascade was used for the coculture experiments. Fibrin alone or in combination with other materials has been used as a biological scaffold for stem or

primary cells to regenerate adipose tissue [Ding *et al.*, 2004], bone [Yang *et al.*, 2012], cardiac tissue [Barscotti *et al.*, 2011; Kim *et al.*, 2012], cartilage [Deponti *et al.*, 2012], nervous tissue [Man *et al.*, 2011] and tendons [Nixon, 2012]. Advantageously, the degree of protein crosslinking in fibrin and therefore its density can be well controlled by varying the mixing ratio of the two compounds of which the scaffold is made of, namely thrombin and fibrinogen. Moreover, fibrin degradation by plasmin, matrix metalloproteinases of endothelial cells can also be controlled by the addition of fibrinolysis inhibitors like for instance aprotinin [Smith *et al.*, 2007, Hedrich *et al.*, 2012].

4. AIM OF THE STUDY

In vitro organ regeneration is still limited by size, since the tissue cells *in vivo* undergo necrosis due to lack of oxygen at distances exceeding 200 μm from a blood vessel. Thus, the need for a vasculature, to deliver nutrients and oxygen and to remove waste materials, is particularly important for *in vitro* engineering of 3D organ and tissue grafts that are thicker than approximately 100 μm .

This thesis addresses the issue of *in vitro* engineering of microvascular networks in fibrin. Microvascular networks are developed *in vitro* from *ad hoc* isolated, primary outgrowth endothelial cells (OECs) cocultured with either undifferentiated ASCs, adipogenically or osteogenically differentiated ASCs in 3D fibrin matrices compared to OEC monoculture control. To do so, two different gel assays are adopted, for which on the one hand *Ibidi- μ -Slides* are used, on the other hand thicker fibrin clots are casted. With the best angiogenesis-supporting type of ASC, different coculture ratios are tested. Further, the microvascular networks generated with and without *Cytodex*TM 1 cellulose beads are compared to each other. The generated networks are evaluated by means of characteristic parameters being the number of tubules, the number of junctions, the total length of tubules and the mean length of tubules using specific software called *AngioSys*TM.

Two dimensional gel assays are evaluated manually by counting and measuring different parameters that characterize the networks. Since three dimensional assays implicate more complex tubular networks, standardized analyses are conducted in those cases using software called *Angiosys*TM.

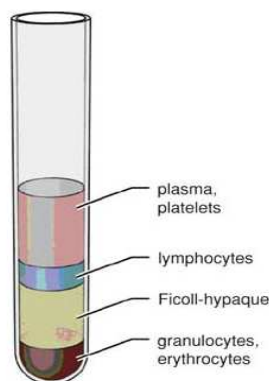
The cells, which contribute to vessel formation are labeled with antibodies against CD31, alpha- smooth muscle actin (α -SMA), matrix metalloproteinase (MMP) 14 and MMP15.

5. MATERIALS AND METHODS

5.1 Outgrowth Endothelial Cell (OEC) Isolation

OECs were isolated from 30 ml human peripheral blood, which was obtained from two male volunteers, one aged 24 years, non-smoker, the other aged 38 years, smoker, both were not receiving any medication and without any clinical diagnosis. The blood was collected after formal consent using 'Vacuette' blood collection set (Greiner Bio-one, Cat.no: 450371) into 'Vacuette' tubes (Greiner Bio-one, Cat.no: 455084), which contained heparin as anticoagulant. Mononuclear cells (MNCs) were isolated from buffy coat, which was separated from the blood by density gradient centrifugation (**Figure 2**).

That was done by diluting the tempered peripheral blood at a ratio of 1:2 with phosphate buffered saline solution without calcium (Ca^{2+}) and magnesium ions (Mg^{2+}), containing 138 mM sodium chloride (NaCl) and 2.7 mM potassium chloride (KCl), pH 7.4 (PBS^-) (Lonza, Cat.no: H21-002). The diluted blood sample was laid onto 30 ml of tempered *Lymphocyte Separation Medium (LSM) 1075*[®] (1.077 g/ml) (PAA, Cat.no: J11-004), by slow pipetting and subsequently centrifuged at 2200 rotations per minute (rpm) for 30 minutes at room temperature (RT) [Böyüm, 1968]. The centrifuge's speed of acceleration and of the brake was adjusted as low as possible, to prevent the density gradient from collapsing.



Source: <http://www.currentprotocols.com/protocol/im0701>

Figure 2: Separation of blood components by density gradient separation. The higher the weight, the deeper will sink the component during centrifugation. Since OECs are mononuclear cells, they reside at the same height as lymphocytes.

The mononuclear cells were collected from the buffy coat, washed with 15 ml PBS⁻ and centrifuged again with 1200 rpm for 5 minutes. The supernatant was discarded; the cell pellet tapped and washed once more with 15 ml PBS⁻. A 30 µl aliquot was taken from this cell suspension for counting the cells in a haematocytometer before the sample was spun down the last time in the centrifuge. The MNC separation was done according to the protocol established by Fuchs *et al.* [Fuchs *et al.*, 2006].

Finally about 10^5 mononuclear cells/cm² were seeded onto tissue culture treated polystyrene 6-well plates (Corning Incorporated) prior coated with a mixture of human placenta derived collagen type I and III (kind gift of Andreas Teuschl, Ludwig Boltzmann Institute for clinical and experimental Traumatology) 1 mg/ml. The cell mixture was suspended in Endothelial Growth Medium (EGM-2), which was composed of Endothelial Basal Medium (EBM-2) (Lonza, Cat.no: CC-3156) supplemented with 10 µg/ml recombinant human fibroblast growth factor B (rhFGF-B), 10 µg/ml vascular endothelial growth factor (VEGF), 10 µg/ml recombinant human epidermal growth factor (rhEGF), 0.1% Ascorbic Acid, 10 µg/ml insulin-like growth factor 1 (r3-IGF-1), 0.1% heparin, Gentamicin sulfate Amphotericin-B (GA-1000), 0.04% Hydrocortisone and 2% fetal calf serum (FCS). All supplements were components of the so called Bullet Kit (Lonza, Cat.no: CC-4176). To enhance endothelial growth additional FCS (Lonza, Cat.no: DE14-870F) was added to a final amount of 5%. First media change was done on the third day after plating out the cells; afterwards, it was performed every second day. After 14 days, the excessive erythrocytes were removed and endothelial cell colonies, exhibiting the characteristic cobblestone-like morphology, could be seen. After 21 days, the colonies had spread over the whole well of a 6-well-plate, thereupon were trypsinized and reseeded on a T25 cell culture flask. The isolated OECs were therefore first split at a ratio of 1:2.7 and termed passage 1 (p1).

The next cell passage was expanded in a T75 cell culture flask and at p3 one third of the cells was used for characterization and the other two thirds were either further expanded for experiments or stored in liquid nitrogen.

5.2 Outgrowth Endothelial Cell Culture

OEC were cultured on cell culture treated surfaces, which were additionally coated with approximately 200 μl of 10 $\mu\text{g}/\text{ml}$ fibronectin (Sigma-Aldrich, Cat.no: F1141-1mG) in EGM-2, 5% FCS. The OEC growth medium was stored at 4°C.

Primary OEC were cryopreserved in 40% dimethyl sulfoxide (DMSO) (Sigma Aldrich, Cat.no: D2650) and stored in liquid nitrogen at -210°C. When needed for experiments, they were thawed and expanded for one passage before use. 10^4 OECs/cm² were finally plated onto cell culture flasks previously coated with fibronectin and expanded. OEC were cultured at 37°C, 95% humidity and 5% carbon dioxide (CO₂); cell growth medium was refreshed every second day. The amount of medium volume per surface area in the culture vessel was approximately 0.2 ml/cm².

Passaging was done regularly when the cells reached 80-90% confluence; the cell density was then between 2×10^4 and 3×10^4 cells/cm². For that, the OEC monolayer was washed with 130 $\mu\text{l}/\text{cm}^2$ PBS⁻ and detached enzymatically from the cell culture flask with 13 $\mu\text{l}/\text{cm}^2$ prewarmed 1x Trypsin-Ethylenediaminetetraacetic acid (TE) (Sigma Aldrich, Cat.no: T4549). Since TE is proteolytically most active at 37°C, the cells were placed in the incubator for 5 minutes during detachment. When the cells' adhesion proteins were digested, they could be seen floating around under the phase contrast microscope. For neutralizing TE, which would otherwise cause cell death, 26 $\mu\text{l}/\text{cm}^2$ of prewarmed EGM-2 were added. In case that exact cell numbers were required for e.g. experiments, the viable cell number of the obtained cell suspension was determined by blue dye exclusion method. For that 10 μl of homogenous cell suspension was aliquoted and mixed with 10 μl of 0.4% weight per volume (w/v) Trypan Blue (Sigma Aldrich, Cat.no: T146). Viable cells appeared white since the stain was not able to penetrate the cell membrane while dead cells appeared blue. The cell concentration was calculated using the following equation:

$$C = N * F * 10^4$$

Eq. 1

Definition of variables:

C cell number [cells/ml]

N Number of counted cells [cells]

F dilution factor [-]

During the cell count, the cell suspension was centrifuged at 1200 rpm for 5 minutes. The cell pellet was finally resuspended and plated out again into the according number of cell culture flasks or wells. For regular expansion, the cells were not counted but split at a ratio of 1:2 or 1:3, depending on the growth rate of the cells. Generally, cell seeding density was approximately 10^4 cells/cm². OECs were used for experiments until p8, in order to avoid any additional variable due to senescence.

5.3 Origin and Culture of Adipose-derived Stem Cells (ASCs)

Adipose-derived stem cells (ASCs) from liposuction material, which was obtained from the Blutzentrale Linz, were isolated as previously described [Wolbank *et al.*, 2007] and cultured in ASC growth medium. It consisted of 88 % Dulbecco's Modified Eagles Medium (DMEM)/ Nutrient mixture Ham F12 (Sigma, Cat.no: D642) - which contained 15mM (4-(2-hydroxyethyl)-1-piperazineethanesulfonic acid (HEPES) and sodium bicarbonate-, 10% FCS, 1% L-glutamine (Sigma-Aldrich, Cat.no: G7513) and 1% Penicillin / Streptomycin (P/S) (Sigma-Aldrich, Cat.no: P4333). ASCs were used at p2 and p3. ASCs were cultured at 37°C, 5% CO₂ and 95% humidity.

5.4 Characterization of OECs and ASCs by Surface Protein Profiling via Fluorescence Activated Cell Sorting (FACS)

Before OECs and ASCs were used in experiments, they were identified by flow cytometry 'Fluorescence Activated Cell Sorting' (FACS), a method, by which cell characteristic surface proteins, so called 'Clusters of Differentiation' (CD), were detected and quantified via specifically binding fluorescence labeled antibodies.

First of all, the cells were harvested from the cell culture vessels using 13 $\mu\text{l}/\text{cm}^2$ 100% (v/v) *Accutase* (PAA, Cat.no: L11-007), a protease solution, which detached the cells more gentle than TE, hence better conserved the cellular surface proteins. After cell detachment and protease neutralization, the cell suspension was centrifuged for 7 minutes at 1,500 rpm and 4°C. The cell pellet was resuspended in 6 ml PBS⁻/0.1% Bovine Serum Albumin (BSA) (Sigma-Aldrich, Cat.no: A9418-10G), at 4°C and centrifuged a second time at the same conditions. Subsequently, the cells were resuspended in 2 ml chilled PBS⁻/0.1% BSA and equally partitioned into ten polypropylene tubes (BD Bioscience) - from then onwards, cells were kept on ice. To each cell sample 7 μl of monoclonal conjugated mouse anti-human antibody were added. OECs were analyzed for CD14, CD31, CD34, CD36, CD45, CD133, CD144, CD146, Tie-2 and VEGFR-2 and ASCs were tested for CD73, CD90 and CD105. As isotype-matched negative control immunoglobins G (IgG) conjugated to phosphatidylethanolamine (IgG-PE) or Fluorescein (IgG-FITC) were used. In **Table 1**, all antibodies, their conjugated fluorophores, their descriptive names and a short description of their functions are listed. After the cell samples were incubated for 30 minutes on ice and in the dark, they were centrifuged for 7 minutes at 1500 rpm. The supernatant containing excess antibody was discarded, the cell pellet was resuspended in 2 ml chilled PBS⁻/0.1% BSA and centrifuged for 5 minutes at 1,500 rpm and 4°C. This washing procedure was repeated once before the cell pellet was resuspended in PBS⁻/0.1% BSA in a final volume of 200 μl . The cells were then ready for analysis in the *BD FACSCalibur Flow Cytometer* (BD Bioscience). The flow cytometry results were processed using *BD FACSDiva software* (BD Bioscience) and the final evaluation was done using *Flowjo software* (TreeStar Inc.).

Table 1: Summary of antibodies used for characterization of OECs and ASCs, including, the conjugated fluorophores, their descriptive names and a short description of their function.

Antibody	Fluorophore	Eventual descriptive names and function of antibodies
IgG	FITC	Isotype Control
IgG	PE	Isotype Control
Characterization of OECs		
CD13		Descriptive Name: Alanine Aminopeptidase; Expressed by committed endothelial cells; often present in tumor angiogenesis [Di Matteo <i>et al.</i> , 2011; Mund <i>et al.</i> , 2011]
CD14	FITC	Functionally implicated in tumor angiogenesis when coexpressed with CD16 and Tie-2 [Hristov <i>et al.</i> , 2009]
CD 31	FITC	Descriptive Name: Platelet Endothelial Cell Adhesion Molecule (PECAM-1); Expressed by platelets, monocytes, neutrophils, and some types of T-cells, and makes up a large portion of endothelial cell intercellular junctions [Yang <i>et al.</i> , 2001]
CD34	PE	Expressed by hemangioblastic cells in combination with VEGFR2; acts as adhesion molecule; [Nielson <i>et al.</i> , 2008]
CD36	PE	Found on platelets, erythrocytes, monocytes, differentiated adipocytes, mammary epithelial cells, spleen cells and some skin microdermal endothelial cells.
CD45	FITC	Descriptive Name: Protein Tyrosine Phosphatase, Receptor type C (PTPRC); hematopoietic origin except erythrocytes & platelets [Leong <i>et al.</i> , 2003]; endothelial characterization: CD45-, CD13+, CD117+, VEGFR2+ [Mund <i>et al.</i> , 2011]
CD61		Descriptive Name: Integrin β -3; expressed by thrombocytes and early endothelial progenitor cells. [Ahrens <i>et al.</i> , 2011]
CD133	PE	Details on function are unknown; expressed by hematopoietic stem cells, endothelial progenitor cells [Corbeil <i>et al.</i> , 2004], glioblastoma, neuronal and glial stem cells [Hristov <i>et al.</i> , 2009], various pediatric brain tumors [Singh <i>et al.</i> , 2003], as well as adult kidney, mammary glands, trachea, salivary glands, placenta, digestive tract, testes, and some other cell types [Mizrak <i>et al.</i> , 2008; Shmelkov <i>et al.</i> , 2005].
CD144	FITC	Descriptive Name: Vascular Endothelial (VE)-Cadherin; necessary for stabilizing and maintaining permeability of newly formed vessels through cohesion and intercellular junctions [Coroda <i>et al.</i> , 2002]
CD146	PE	Descriptive Name: Melanoma Cell Adhesion Molecule (MCAM); Expressed by committed vascularizing cells [Mund <i>et al.</i> , 2011]
Tie-2	PE	Angiopoietin-1 Receptor; Expressed by committed vascularizing cells; angiopoietins are protein growth factors promoting angiogenesis, which bind to Tie-2 [Gu <i>et al.</i> , 2011]
VEGFR-2	PE	Descriptive Name: Kinase Insert Domain Receptor (KDR) or Fetal Liver Kinase (Flk) -1; expressed by committed endothelial cells [Arao <i>et al.</i> , 2011]
Characterization of ASCs		
CD73	PE	In combination with CD105 and CD90, CD73 is a characteristic marker for hematopoietic stem cells [Majeti <i>et al.</i> , 2007], mesenchymal stem cells
CD90	FITC	See CD73
CD105	FITC	Descriptive Name: Endoglin; see CD73
HLA - DR		Human Leukocyte Antigen; it is a Major Histocompatibility Complex (MHC) class II cell surface receptor expressed by all nucleated cells.
HLA - ABC		Three isoforms of Human Leukocyte Antigen; it is a Major Histocompatibility Complex (MHC) class I cell surface receptor expressed by all nucleated cells.

5.5 ASC Differentiation into the Adipogenic and Osteogenic Lineage

ASCs were differentiated into the adipogenic and osteogenic lineage by changing ASC control medium to osteogenic or adipogenic differentiation medium at about 50% confluence and then culturing them for 21 days without splitting, while the respective medium was refreshed every second day. The adipogenic differentiation medium consisted of high glucose DMEM, with 4500 g/l (Sigma-Aldrich, Cat.no: D6546),

supplemented with 10% FCS, 1% L-Glutamine, 1% Penicillin / Streptomycin (P/S), 1 μ M Dexamethasone (Sigma-Aldrich, Cat.no: D2915), 0.5 mM 3-isobutyl-1-methylxanthine (IBMX, Sigma-Aldrich, Cat.no: I7018), 0.5 μ M Hydrocortisone (Stemcell Technologies, Cat.no: 07904) and 0.06 mM Indomethacin (Sigma-Aldrich, Cat.no: I7378). The osteogenic differentiation medium consisted of DMEM with 1000 g/l glucose, containing 10% FCS, 1% L-Glutamine, 1% P/S, 0.1 μ M Dexamethasone, 150 μ M Ascorbic Acid (Sigma-Aldrich, Cat.no: 49752) and 10mM beta-Glycerophosphate (Stemcell Technologies, Cat.no: 05406). To examine the mineralization in the living culture, which takes place during osteogenic differentiation, Xylenol Orange (Fluka, Cat.no: 52097-1G) [Wang *et al.*, 2006] was added at a final concentration of 20 μ M overnight. Parallel to differentiation, ASCs of the same batch and passage were cultured in ASC growth medium as control. After 3 weeks of culture, the cells were detached with 13 μ l/cm² 100% (v/v) *Accutase* for at least 5 minutes at 37°C and eventually scrapping. Thereafter they were counted, centrifuged at 1,200 rpm for 5 minutes and finally resuspended in appropriate volumes of EGM-2 to attain same cell concentrations.

To test, whether the undifferentiated as well as the differentiated ASCs produced angiogenesis-supporting cytokines, 15 ml of consumed culture medium of each monolayer and 15 ml of fresh EGM-2 were collected and analyzed via Enzyme-Linked Immunosorbent Assay (ELISA) for bFGF and VEGF concentrations.

After appropriate amounts of ASCs were used for fibrin clot and *Ibidi μ -slide* experiments, the rests of undifferentiated as well as osteogenically and adipogenically differentiated ASCs were distributed over 9 wells of a 12-well-plate as shown in **Figure 3** and cultured in parallel to those seeded into fibrin for further 14 days.

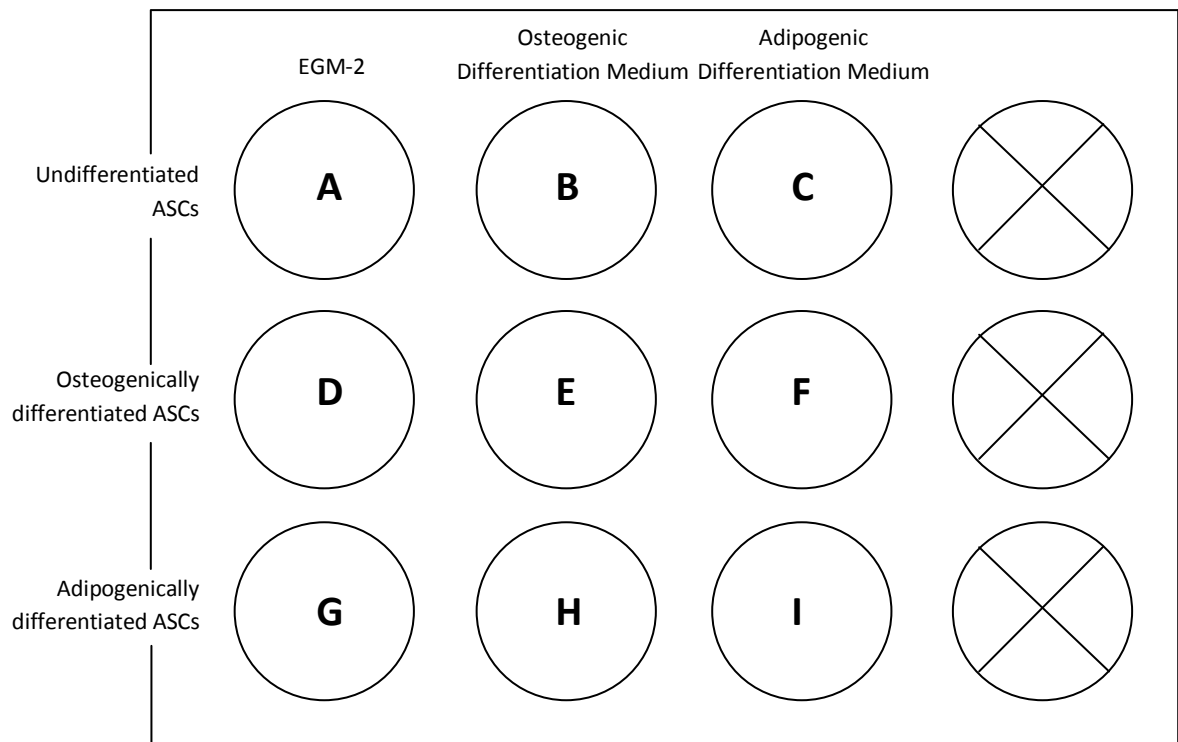


Figure 3: Scheme of 12-well plate for monolayer controls of undifferentiated as well as osteogenically and adipogenically differentiated ASCs, maintained in parallel to coculture experiments in fibrin. The same numbers of undifferentiated, osteogenically and adipogenically differentiated ASCs were split into three and distributed over three wells respectively. After one day of culture in EGM-2, two wells of each condition were changed to osteogenic and adipogenic differentiation medium. Undifferentiated, osteogenically differentiated and adipogenically differentiated ASCs were cultured in EGM-2 in the wells A, D and G, respectively. In the wells B, E and H, the three cell types were cultured in osteogenic differentiation medium and in C, F and I in adipogenic differentiation medium. Medium refreshment was performed every second day.

5.6 Cell Seeding onto *Cytodex*TM 1 Cellulose Beads

Basically, two different methods of OEC/ASC cocultures in fibrin were compared: either OECs were seeded onto *Cytodex*TM 1 cellulose beads (GE Healthcare, Cat.no: 17-0448-01) one day before they were transferred together with ASCs into fibrin, or they were, just like the ASCs, transferred to fibrin as a single cell suspension.

*Cytodex*TM 1 beads were stored at room temperature in PBS⁻ at a concentration of 20,000 beads/ml and were washed and equilibrated in EGM-2 before OECs were seeded onto them. Depending on the size of the experiments, either 1 or 2 ml of the suspended beads

was pipetted into a vial and left without motion until the beads had settled down. The supernatant PBS⁻ was aspirated and the beads were resuspended in a defined volume of EGM-2. This procedure was repeated once before the cell suspension was finally added to the beads. The bead concentration was calculated as follows:

$$\text{Conc}_{\text{actual}} = (\text{Conc}_{\text{stock}} * \text{Vol}_{\text{taken}}) / \text{Vol}_{\text{actual}} \quad \text{Eq. 2}$$

$\text{Conc}_{\text{actual}}$ Concentration of *Cytodex*TM 1 beads suspended in EGM-2; calculated after two wash steps

C_{stock} Concentration of *Cytodex*TM 1 stock solution; 20 000 cells/ml

V_{taken} Volume taken of *Cytodex*TM 1 stock solution

V_{actual} Volume of *Cytodex*TM 1 beads suspended in EGM-2; determined after two wash steps

After determining the *Cytodex*TM 1 bead surface (Eq. 3), the amount of OECs needed for a confluent monolayer was calculated. From experience 40,000 OECs/cm² create a confluent monolayer. By multiplying the bead surface and the cell density at confluence, the cell number needed for confluent monolayers on the beads was determined (Eq. 4). The cell seeding density for each of the mentioned experiments was therefore approximately 100 cells/bead and the overall number of OECs present in a fibrin clot containing 200 beads was 20,000 OECs (Eq. 5).

Calculation of surface area of a *Cytodex*TM 1 cellulose bead:

$$\text{O}_{\text{sphere}} = d^2 \times \pi = (2.9 \times 10^{-2})^2 \times \pi = 0.00264 \text{ cm}^2 \quad \text{Eq. 3}$$

O_{sphere} Surface area of a sphere

d diameter of the sphere, in case of *Cytodex*TM 1 cellulose beads ~ 0.029 cm

Calculation of cell number on a *Cytodex*TM 1 cellulose bead with an assumed cell density of 4×10^4 cells/cm²:

$$4 \times 10^4 \text{ cells/cm}^2 \times 0.00264 \text{ cm}^2 = 105.7 \text{ cells} \quad \text{Eq. 4}$$

Calculation of the number of OECs/clot

$$100 \text{ OECs/bead} \times 200 \text{ beads/clot} = 20\,000 \text{ OECs} \quad \text{Eq. 5}$$

The mixture of OECs and beads was transferred into a T25 cell culture flask and placed in a vertical position into the incubator; an explaining scheme is illustrated in **Figure 4**. The cell-bead suspension was shaken every 30 minutes for the next 4 hours in order to give cells that fell to the bottom of the flask some more chances to adhere to the beads. Finally, the cell-bead-suspension was incubated at 37°C, 95% humidity and 5% CO₂ overnight.

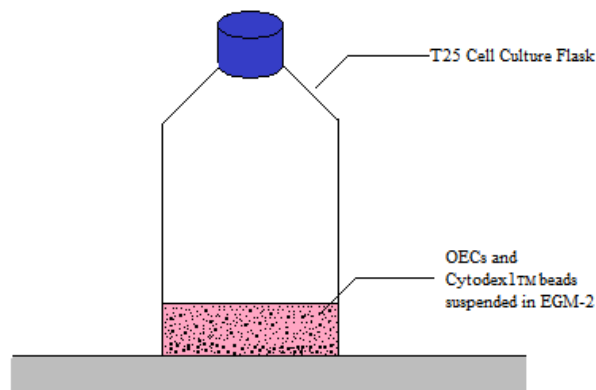


Figure 4: Scheme of how OECs were seeded onto cellulose beads. For the experiments described in this study, approximately 0.5 to 1 ml of *Cytodex*TM 1 cellulose beads, which were approximately 10^4 to 2×10^4 beads, were aliquoted. After they were washed twice with EGM-2, they were added together with approximately 200 OECs/bead into a T25 cell culture flask, which was placed vertically into the incubator for 4 hours. Every 30 minutes, the flask was manually inverted to redistribute the sunken cells and beads.

5.7 Inoculation and Coculture of OECs together with Undifferentiated, Adipogenically and Osteogenically Differentiated ASCs in Fibrin

In case of OECs seeded onto *Cytodex*TM 1 beads beforehand, approximately 4×10^4 OECs/ml (fibrin) were inoculated and coculture ratios of 1:1, 5:1 and 10:1 (OEC:ASC) were investigated. The calculated OEC concentration was based on the assumption that all cells adhered to the beads, which would give approximately 200 cells/bead. The bead concentration was ascertained by counting them in a defined volume under the phase contrast microscope. Cells used for coculture were undifferentiated ASCs, osteogenically and adipogenically differentiated ASCs. The fibrin clots had a final volume of 200 μ l and were composed of 2.5 mg/ml fibrinogen (Baxter) and 0.2 Units/ml Thrombin (Baxter).

In case of OECs added to the fibrin clots as cell suspension, 10^6 OECs/ml was inoculated to achieve a similar degree of microvascular tube formation. The coculture ratios of OECs to ASCs investigated were 1:1, 2:1, 5:1 and 10:1; the final volume of the clots was 100 μ l and they were again composed of 2.5 mg/ml fibrinogen (Baxter) and 0.2 Units/ml Thrombin (Baxter).

Prior to casting, 100 or 50 μ l of 0.4 Units/ml thrombin solution – 4 Units/ml thrombin stock was diluted 1:1 with calcium chloride (CaCl_2) –and 100 or 50 μ l of 5 mg/ml fibrinogen solution including the appropriate number of OECs on beads or suspended cells, respectively, and coculture cells were aliquoted into Eppendorf® tubes. A scheme of how the contents were partitioned before casting is illustrated in **Figure 5**. After fibrinogen, EGM-2, OECs and the coculture cells as well as thrombin and CaCl_2 were prepared, the contents of the two Eppendorf® tubes were mixed by gently pipetting up and down twice. The 200 or 100 μ l mixtures, respectively, was finally casted onto round, sterile cover slips with diameters of 15 mm (BD Bioscience), that had been laid into the wells of a 12-well-plate. The most critical step during fibrin clot casting was time, since fibrinogen and thrombin coagulated a few seconds after mixing.

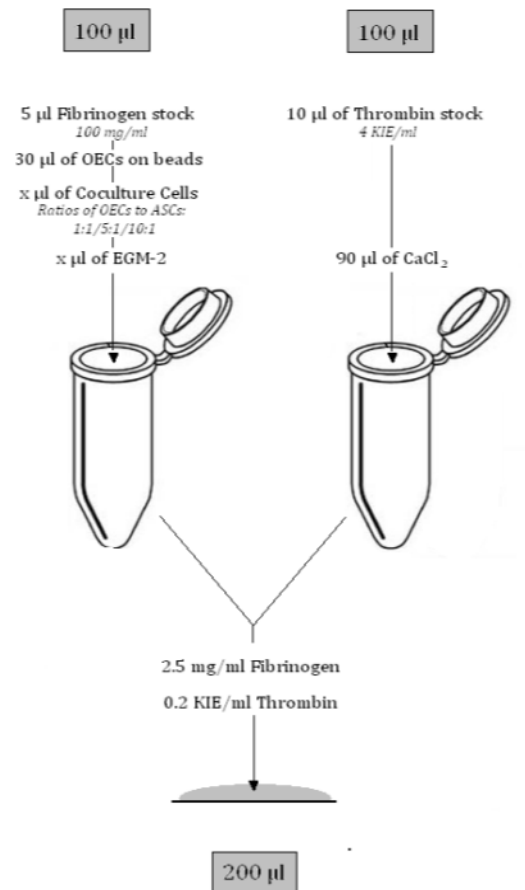


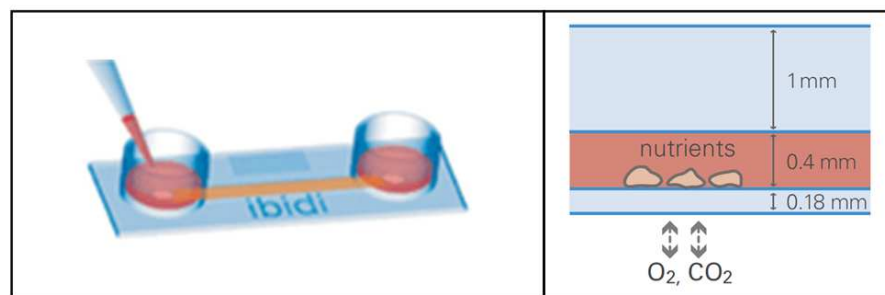
Figure 5: Mixing scheme for fibrin clot casting. In one Eppendorf® tube, fibrinogen stock, OECs with or without beads, single suspended coculture cells and EGM-2 were mixed together while the other one contained only thrombin stock diluted with the appropriate amount of CaCl₂. The final fibrin clot had a volume of 200 µl, a fibrinogen concentration of 2.5 mg/ml and a thrombin concentration of 0.2 KIE/ml.

The fibrin clots were placed for approximately 30 minutes into the incubator at 37°C to ensure that the fibrin matrix was crosslinked before EGM-2 was added. To prevent the fibrin from digestion by the cells, the medium was supplemented with the fibrinolysis inhibitor aprotinin (Baxter, Cat.no: VNL2G007) at a concentration of 100 Kallikrein-Inhibitor-Unit (KIU)/ml.

5.8 Inoculation and Coculture of OECs together with Undifferentiated, Adipogenically and Osteogenically Differentiated ASCs in Ibidi Slides

Besides fibrin clots, so called “*Ibidi µ-Slides I*” (I.B.L., Cat.no: 80106) (**Figure 6**) were also used to coculture OECs with ASCs in fibrin. An *Ibidi µ-Slide* can be described as a

combination of a cell culture dish and a cover slip with a flow channel. The main advantage of those slides was their compartment with a total volume of 100 μl and a height of 400 μm (**Figure 6**, right), which was optimal for investigation of microvascular capillaries under the phase contrast microscope. In this system, only OECs on beads, but not OECs in suspension, were cocultured with undifferentiated ASCs, osteogenically and adipogenically differentiated ASCs. The tested ratios and the preparation procedure was generally the same as that for casting fibrin clots, which was described above in 0.



Source: <http://www.ibl.or.at/slides.pdf>

Figure 6: Scheme of Ibidi- μ -slide. On the right hand side, the whole μ -slide is illustrated. 500 μl of culture medium is added to each compartment, which diffuses through the channel. On the right hand image, gas exchanging through the base of the μ -slide is schematically shown. Owing to the flat compartment, which is only 0.4 mm high, the cells cultured in fibrin can still be investigated through the light microscope, since most of them are located within the focal distance and do not interfere with objects in the focal plane.

For cell nutrition, 0.5 ml EGM-2 was added to each of two compartments of the *Ibidi μ -Slides* (see **Figure 6**, left) and exchanged as common every second day. Since gas exchange, occurred via the bottom of the slides, they were placed not directly onto the incubator shelf but onto pipette tip racks which allowed gas diffusion through the slide's base.

5.9 Immunoblotting

To visualize tubules, they were stained with different conjugated antibodies. Endothelial cell junctions were incubated in anti-CD31-FITC; anti- α -SMA (Sigma-Aldrich, Cat.no: A5228) was used to determine, whether ASCs differentiated into pericytes; the anti-Matrix Metalloproteinase (MMP) 14 (Millipore, Cat.no: AB6004) and anti-MMP 15

(Chemicon, Cat.no: AB8555) were used to illustrate that OECs actively degraded fibrin matrix to elongate their tubules.

Before staining, the medium was discarded and the fibrin clots were transferred from 12-well plates to 24-well plates and washed with 1 ml chilled PBS⁻/0.1% BSA on the shaker. After 5 minutes, PBS⁻/0.1% BSA was discarded and the wash procedure was repeated twice. Subsequently, the cells in the clots were fixed in 1 ml of 4% paraformaldehyde (PFA) during incubation overnight at 4°C before the clots were washed three times for 5 minutes with 1 ml chilled PBS⁻/0.1% BSA at RT on the shaker.

Afterwards, to one part of the clots 200 µl of anti-CD31-FITC, diluted 1:100 with PBS⁻/0.1% BSA, was added and incubated for at least 6 hours at RT on the shaker. Starting with the addition of the first fluorophore-conjugated antibody until microscopy, the 24-well plate containing the fibrin clots was wrapped with aluminum foil to protect the cells from light, which would otherwise reduce the fluorescence signal intensity. After the clots were again washed three times, 200 µl of 1:100 diluted mouse anti-human alpha-SMA primary antibody was added for at least 3 hours at RT on the shaker. Thereafter, 1 µl of 1:100 diluted secondary goat anti-mouse Alexa Fluor® 594 nm (Invitrogen, Cat.no: A21044) antibody was added to the primary antibody solution onto the fibrin clots and again incubated on the shaker overnight.

To the second part of the clots, 200 µl of anti-MMP15 antibody (also called membrane type (MT) 2- MMP), diluted 1:250 and to the third part, 200 µl of anti-MMP14 antibody (or MT1-MMP), diluted 1:250 were added overnight; all were left at RT on the shaker. After three washings in again PBS⁻/0.1% BSA, the clots stained against MMP15 were incubated in secondary human anti-rabbit Alexa Fluor® 594nm antibody and those stained against MMP14 in secondary human anti rabbit Alexa Fluor® 488nm antibody, respectively, in both cases, the clots were incubated for 5 hours.

After incubation, excess antibody was removed during three final washing steps before the clots were incubated in 200 µl of 1:1000 diluted 4',6-Diamidin-2-phenylindol (DAPI)

for 5 minutes at RT, on the shaker. The clots were washed once more before they could finally be examined with an epifluorescence microscope (Leica DMI6000B).

5.10 Investigation of different OEC:ASC Coculture Ratios and the Tubular Network Formation with and without *Cytodex*TM 1 Cellulose Beads

The OEC concentration was held constant in each clot at 10^6 cells/ml, which were 2×10^5 OECs/clot, since they had a volume of 200 μ l. Hence the ASC concentration was varied to achieve following coculture ratios: 1:1, 2:1, 5:1 and 20:1. Therefore 2×10^5 , 10^5 , 4×10^4 and 10^4 ASCs respectively were added to the clots. Negative control was OEC monoculture in fibrin clots at 10^6 cells/ml seeding concentration. Those four coculture ratios were compared in clots with OECs, initially seeded onto beads and in clots without any beads. All coculture systems were maintained for 14 days.

5.11 Non-Standardized Quantification of Tubules in *Ibidi- μ -Slides*

The quality of the microtubular networks generated in *Ibidi- μ -Slides* with OECs that were seeded onto *Cytodex*TM 1 cellulose beads was evaluated by three independent persons without any knowledge of this experiment. They received photo series' depicting the whole area of the *Ibidi- μ -Slides* containing OECs cocultured with undifferentiated ASCs, osteogenically differentiated ASCs and adipogenically differentiated ASCs at two different OEC:ASC coculture ratios, namely 3.5:1 and 1:1. Thus, in sum 6 photo series were evaluated. The evaluation parameters were A) the total number of beads, B) the number of beads, from which tubular structures sprout and C) the number of sprouts per bead. Also D) the sprout lengths were determined by measuring between two junctions, two beads or between a junction and a bead, respectively.

5.12 Standardized Quantification of Stained Tubules

By increasing the dimension from gel assays in *Ibidi-μ-Slides* to gel assays in fibrin clots, also the complexity of the generated tubular structures was increased. Moreover, more different conditions were investigated, namely OECs cocultured with undifferentiated ASCs at the ratios 1:1, 2:1, 5:1 and 20:1 as well as with and without *Cytodex*TM 1 cellulose beads. The produced microvascular networks were compared using software called *Angiosys*TM (TCS Cellworks), which analyzed the fluorescence images with respect to four different parameters: A) number of tubules, B) mean length of tubules, C) total length of tubules and D) number of junctions. To achieve a correct quantification, the fluorescence images were standardized using Adobe Photoshop Elements 9 (PSE 9) in five steps. The exact commands and their functions are summarized in **Table 2**.

Table 2: Summary of actions taken in PSE9 and the according commands as well as descriptions of the manual adjustments done for fluorescence image processing.

	Action	Commands	Manual Adjustment
1	Change to grey scale	Bild → Modus → Graustufen	
2	Invert black and white	Tonwertkorrektur → Tonwertumfang	The black regulator was adjusted to the right side and the white one to the left side of the spectrum peak
3	Adjust autolevels	Tonwertkorrektur → Tonwertspreizung	The regulators were adjusted close to the spectrum peak ascent and descent which caused a bracing of the actual grey scale spectrum upon the whole black-white spectrum. The darkest actual grey value therefore appeared black in the new image and the lightest one white.
4	Adjust	Schärfe einstellen: Stärke 500%	

	sharpness	(max); Radius: 64 Pixel (max)	
5	Manual correction		Overexposed fluorescence signals as well as signals of single cells were manually deleted using the PSE9 tool 'rubber'.

5.1 Placenta Decellularization

In addition to the generation of microvascular networks from endothelial cells cocultured with different cell types in fibrin, which is investigated in this thesis, also the approach of developing such networks in already existing tissue patches was taken into consideration. For that, a piece of placental tissue with an approximate area of 144 cm² was excised and released from muscular tissue adhering to the inner side of the placenta. On this piece, the two largest vessels were determined and connected to tubes via two permanent venous catheters. Through these tubes, different decellularizing agents (**Table 3**) were pumped through the placental vessels for 13 days for different periods of time (

). Antibiotics/antimycotics (ABAM) and phenylmethylsulfonylfluoride (PMSF) were added to buffers A, B and C to prevent them from severe bacterial or fungal contamination while PMSF acts as protease inhibitor.

The decellularization buffers were exchanged by fresh ones daily. The decellularization took place in a cold room at 4°C. Only during the enzymatic digestions, for which DNase and RNase were added for 24 hours, the tissue was placed into an incubator adjusted to 37°C, since the proteinases are most active at 37°C. Leakages of the vessels were sealed by the application of a physiological glue, which consisted of 10% glutaraldehyde (Sigma-Aldrich) mixed with human albumin "Behring" 20% infusion solution (CSL Behring GmbH). Since this mixture crosslinked, it had to be applied quickly.

Table 3: Compositions of decellularizing agents.

Buffer A		Buffer B		Buffer C		Buffer D		Enzymatic digestion	
pH 8.00		pH 8.00		pH not adjusted		pH not adjusted		pH not adjusted	
10 mM	Tris Base	50 mM	Tris Base	50 mM	Tris Base	50 mM	Tris Base	55 mM	Na ₂ HPO ₄
50 mM	EDTA	1.5 M	KCl	1%	Lauroyl Sarcosinate	1%	Triton X-100	17 mM	KH ₂ PO ₄
1%	PMSF	5 mM	EDTA					4.9 mM	MgSO ₄ x 7 H ₂ O
1%	ABAM	1%	Lauroyl Sarcosinate	1%	PMSF			15 000 U	DNase Type I
				1%	ABAM			12.5 mg	RNase Type IIIA
			1%	PMSF					
			1%	ABAM					

Table 4: Chronologic order of decellularizing agents pumped through the placental vessels. The agents were exchanged by fresh ones daily and decellularization occurred at room temperature, except for the enzymatic digestions, which occurred at 37°C.

Day	Decellularizing agent
1	Buffer A
2	Buffer A
3	Buffer B
4	Buffer B
5	Buffer C
6	Buffer C
7	Buffer C
8	Enzymatic digestion
9	Buffer D
10	Buffer D
11	Enzymatic digestion
12	Buffer D
13	Buffer D

Whether the placental tissue was successfully decellularized or not was determined by hematoxylin and eosin (H&E) staining of microtome-cut paraffin slices (Baker, 1962).

6. RESULTS

6.1 Outgrowth Endothelial Cell Isolation

On an average, it took 10 days for first endothelial cell colonies to establish from the EPC fraction within the mononuclear cell population. OECs were phenotypically recognized by their characteristic cobble-stone like morphology (**Figure 7**).

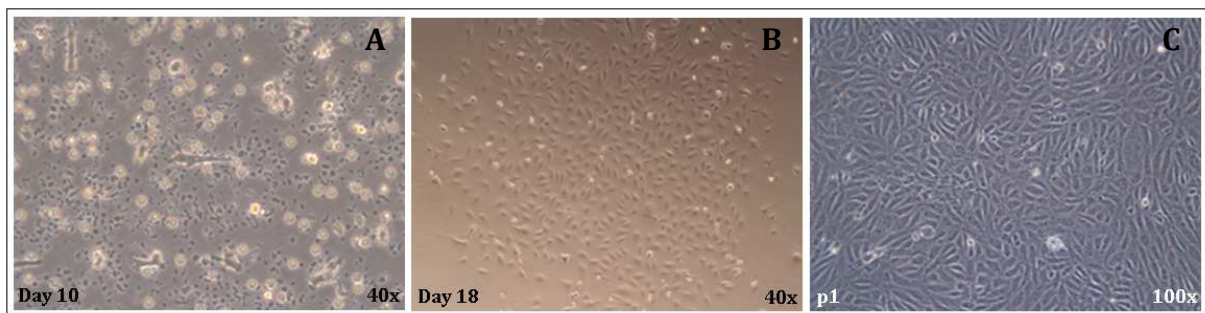


Figure 7: Endothelial cell isolation from peripheral blood. A) First adhering cells could be seen 10 days after plating out the separated, mononuclear blood cells. B) After 18 days, homogenous cell colonies have established. C) Characteristic cobble stone morphology of isolated and expanded cells.

6.2 Characterization of OECs and ASCs by Surface Protein Profiling via Fluorescence Activated Cell Sorting (FACS)

The isolated cells were characterized by flow cytometry at passage 5. As can be seen in **Figure 8**, 100% of the cells expressed the endothelial markers CD31, CD146, CD73 and CD13. Approximately 98% expressed VE-Cadherin, VEGFR2, and β -integrin (CD61), the latest being suggested to be characteristic for early endothelial progenitor cells [Ahrens *et al.*, 2011]. The cells were partly positive for CD34, though they reduced expression at later passages. The high expression of CD146, CD31, VE-Cadherin and VEGFR2 proves the true endothelial nature while the low expression of Tie-2 and CD133 indicates that the cells are not progenitors any more but rather fully differentiated. Moreover, the analysed cells were negative for the pan-hematopoietic and the leukocyte marker CD45 and CD14, respectively.

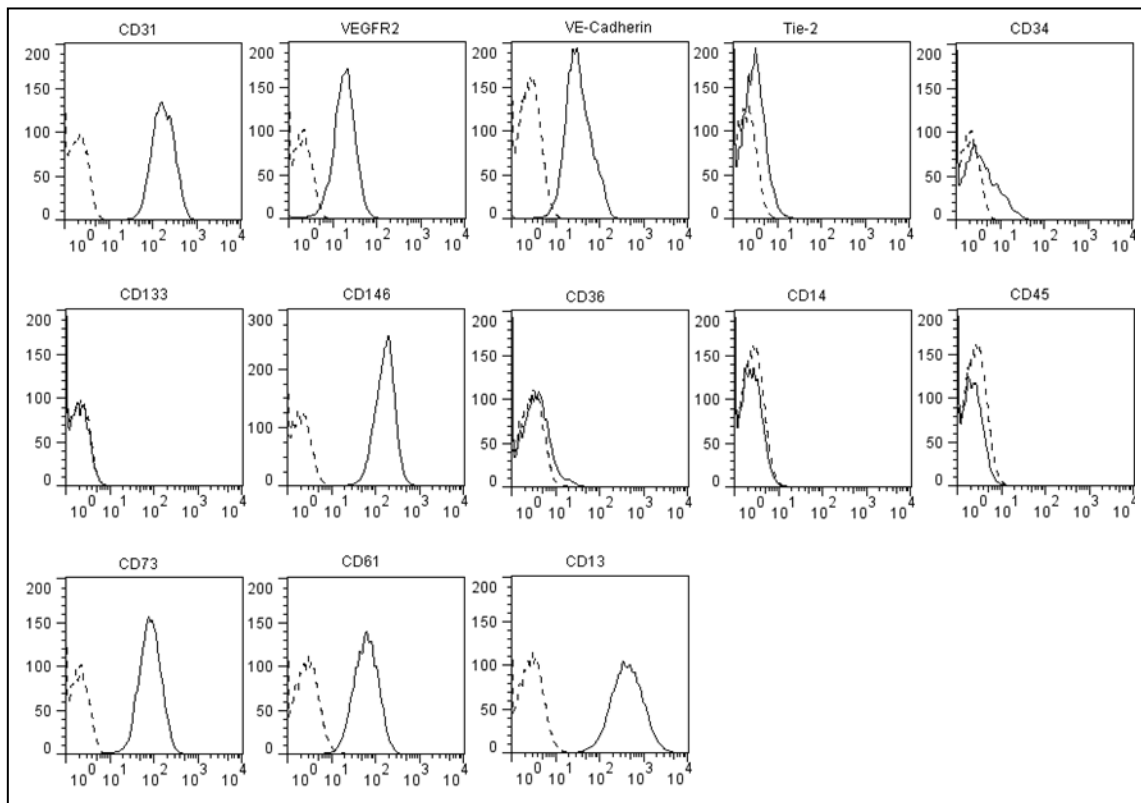


Figure 8: Flow cytometry results showing a characteristic OEC surface marker profile. Regarding characteristic surface markers for endothelial progenitors, only approximately 20% of the cells express Tie-2 and CD34 while they lack CD133, CD36, CD14 and CD45. Instead, they show characteristic outgrowth endothelial cell markers: 100% of the cells express CD31, CD146, CD73, CD61 and CD13; approximately 98% of them express VEGFR2 and VE-Cadherin.

From those flow cytometry results, it can be concluded, that the isolated cells are not progenitor endothelial cells but rather already differentiated outgrowth endothelial cells.

In contrast to the endothelial cells, 100% of the ASCs expressed CD73, 98% CD90 and HLA-ABC, 95% CD105 and approximately 75% expressed CD146. The cells did not express CD45, CD31 and CD34 and only about 10% expressed CD14 and HLA-DR (**Figure 9**). The combined expression of CD73, CD90 and CD105 together with the absence of CD45 and CD34 generally confirms the stemness of the analyzed cells. The absence of CD14 can be interpreted as that these cells do not have hematopoietic origin, while the complete absence of CD31 proves that no committed endothelial cells are present in this cell population. The presence of HLA-ABC indicates the expression of MHC class I and the signal of the anti-CD146 antibody, that part of the cell population has an endothelial progenitor potential. However, it was found, that the ASCs lost CD146 during passaging (data not shown).

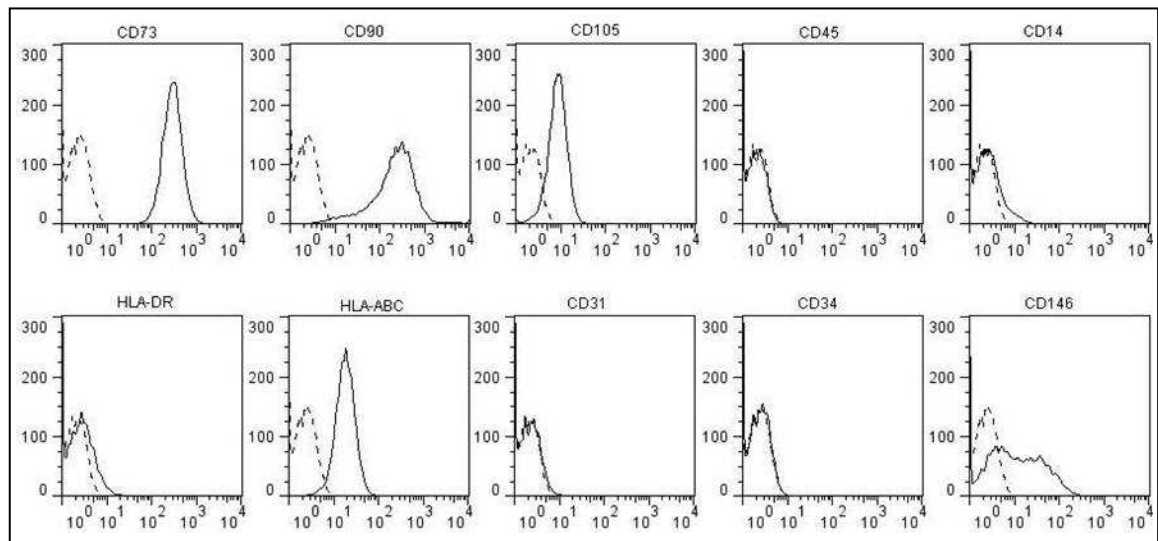


Figure 9: FACS results showing the ASC surface marker profile.

6.3 Differentiation into the Adipogenic and Osteogenic Lineage

ASCs were allowed to differentiate for 21 days which was documented by photographs taken through the phase contrast microscope (**Figure 10**). ASCs cultured in adipogenic differentiation medium already formed first oil containing vacuoles after 2 days, as can be seen on the upper left image of **Figure 10**, while characteristic mineralized nodules were seen after 7 days of culture in osteogenic differentiation medium.

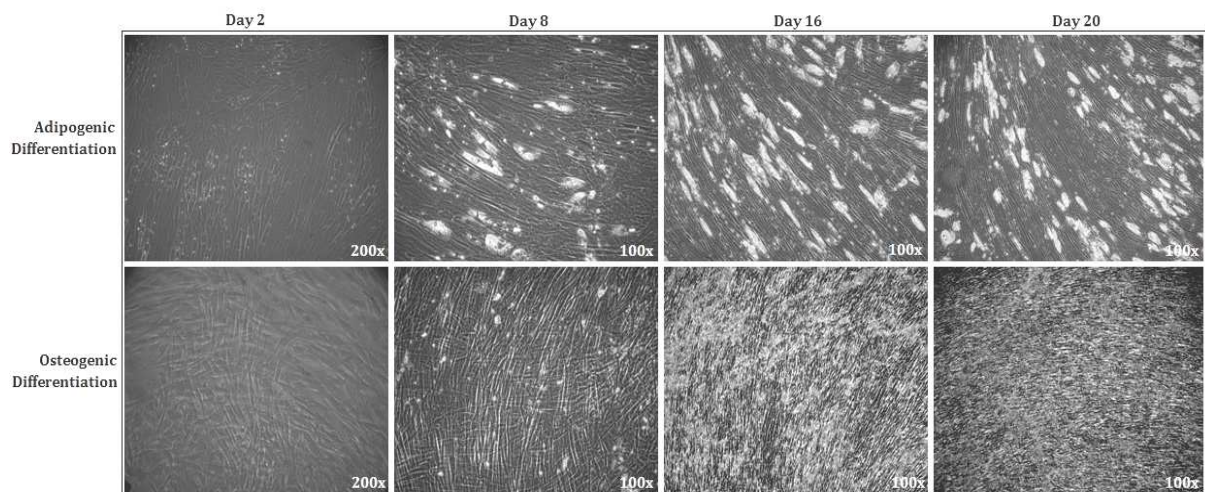


Figure 10: Adipogenic and osteogenic differentiation of ASCs. The days were numbered, starting with Day 0, when ASC growth medium was changed to differentiation medium.

Osteogenic differentiation was proven to be successful on day 20 by Xylenol Orange, which chelated with Ca^{2+} and Mg^{2+} ions of the mineralized nodules and emitted orange light when excited with light at about 546nm (**Figure 11**).

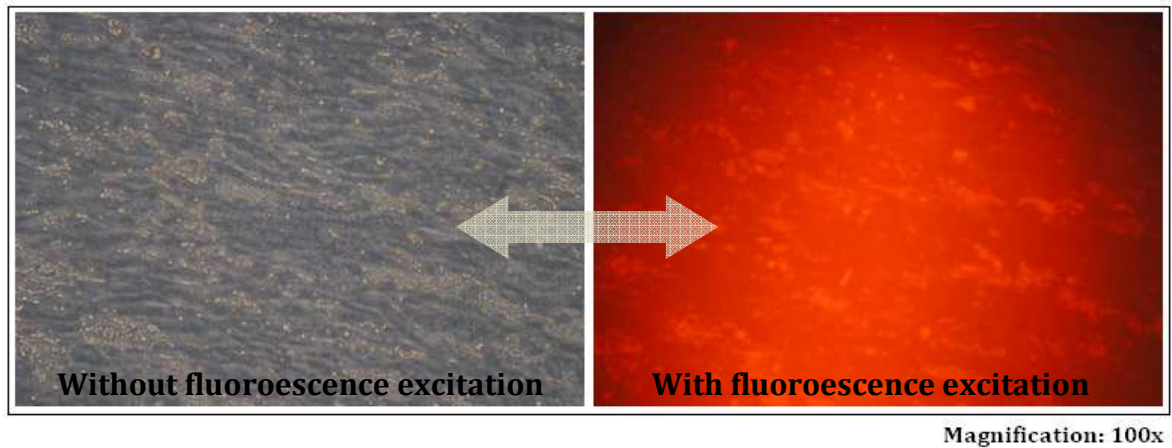


Figure 11: Osteogenic differentiation was proven to be successful by Xylenol Orange staining after 20 days of culture in osteogenic differentiation medium. The left image shows a light microscope image of the differentiated ASC monolayer. The right image depicts the same area illuminated with light at a wavelength of 546 nm. Comparing both images, it can be said, that the white nodules on the left emit a fluorescence signal on the right image, which proves their mineral content.

The VEGF concentrations, determined by ELISA are plotted in **Figure 12**. Fresh EGM-2 contains the lowest concentration of VEGF compared to the consumed ASC growth medium, the osteogenic and the adipogenic differentiation media. The VEGF concentrations were highest in the media of osteogenically and adipogenically differentiating ASCs, namely 1615 and 1250 pg/ml, respectively.

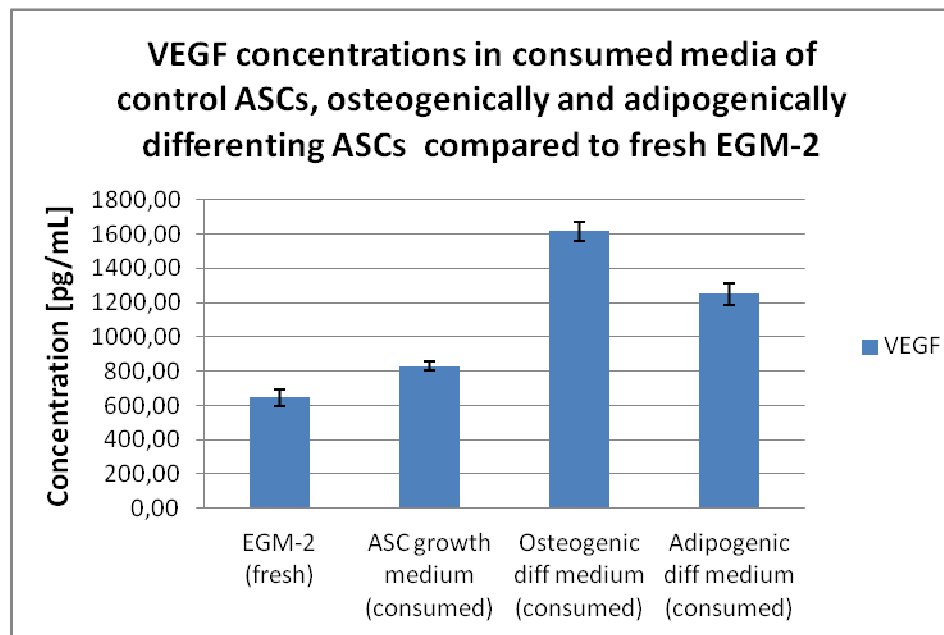


Figure 12: ELISA of fresh EGM-2 compared to consumed media of undifferentiated, osteogenically and adipogenically differentiating ASCs after 3 days on the confluent monolayers. VEGF concentration was the lowest in EGM-2 with about 650 pg/ml, while consumed osteogenic differentiation medium contained the highest concentration, namely approximately 1600 pg/ml.

As controls to the cells cultured in fibrin, ASCs that were previously cultured for three weeks in adipogenic or osteogenic differentiation medium or ASC growth medium were reseeded on cell culture wells. **Figure 13** comprises phase contrast microscope images of the ASCs one day after reseeding (“Day 1”).

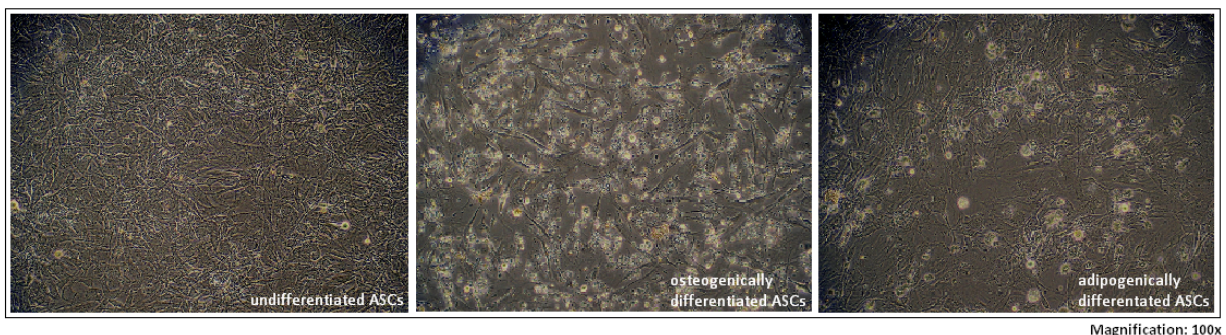


Figure 13: ASCs, p4 were cultured for three weeks in either ASC growth medium, osteogenic or adipogenic differentiation medium thereafter enzymatically detached and reseeded; the images above show the ASCs one day after reseeding. Most cells survived and adhered in case of the undifferentiated ASCs. A lot of cell debris and loose mineralization nodules are present with the osteogenically differentiated ASCs. Also many dead cells can be seen on the right image, which shows adipogenically differentiated ASCs. However, approximately the same number of cells of the differentiations adhered.

After 20 days in culture, all cells recovered and expanded to confluent monolayers as can be seen in **Figure 14**. Originally undifferentiated ASCs did neither lose their adipogenic nor their osteogenic differentiation potential although they were previously maintained for three weeks at full confluence (**Figure 14B and C**). Moreover, ASCs that were cultured

for three weeks in osteogenic differentiation medium could further be differentiated into the osteogenic lineage (**Figure 14E**) and also showed characteristic signs of differentiation into the adipogenic lineage (**Figure 14F**) upon culture in the respective medium. The same but *vice versa* was observed with originally adipogenically differentiated ASCs (**Figure 14H and I**), although those cells produced significantly less mineralized matrix or accordingly oil droplets, which might be a sign of a decreased differentiation potential. On the other hand, there were still a few fat vacuoles and mineralized nodules, respectively, present in the previously differentiated ASCs when cultured in EGM-2 for three further weeks (**Figure 14D and G**).

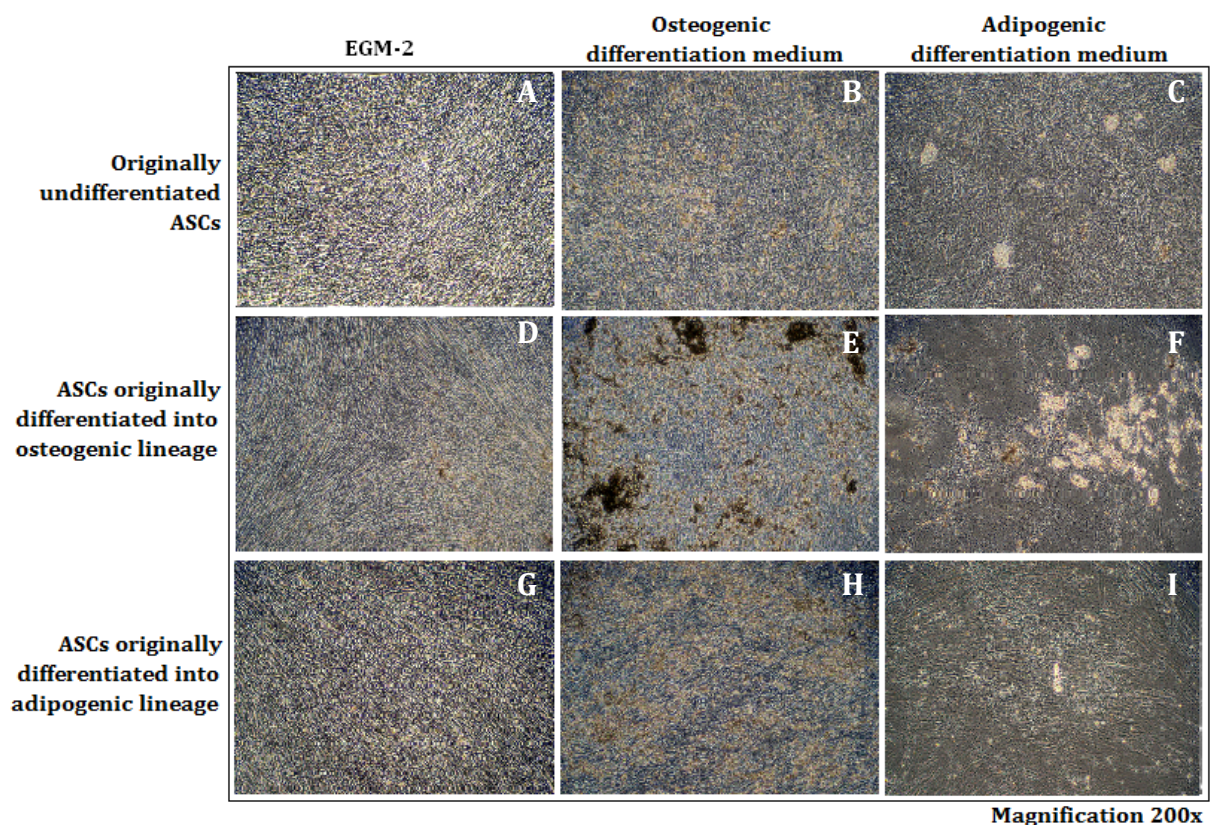


Figure 14: ASCs, which were previously cultured in ASC growth medium, osteogenic or adipogenic differentiation medium for 3 weeks, then detached, reseeded and cultured for another 18 days in EGM-2, osteogenic or adipogenic differentiation medium, respectively. **A-C:** Originally undifferentiated ASCs produced mineralized nodules as well as oil-droplets-containing vacuoles. **D-F:** The mineralized matrix was not resorbed by originally osteogenically differentiated ASCs during culture in EGM-2, while they produced further mineralized nodules upon culture in osteogenic differentiation medium as well as fat droplets upon culture in adipogenic differentiation medium. **G-I:** ASCs differentiated into the adipogenic lineage recovered and could also be triggered to differentiate into the osteogenic lineage. Compared to the originally osteogenically differentiated ASCs, they produced significantly less oil droplets or mineralized matrix, which indicates, that the adipogenically differentiated ASCs have lost some of their differentiation potential.

6.4 Coculture of OECs and ASCs in Fibrin

6.4.1 Coculture of OECs with Undifferentiated ASCs, Osteogenically and Adipogenically Differentiated ASCs compared to OEC Monoculture in Fibrin

Prior to starting the coculture of OECs with different cell types, they were seeded onto *Cytodex*TM 1 cellulose beads. As can be seen in **Figure 15**, the beads were completely covered with OECs when they were casted into fibrin.

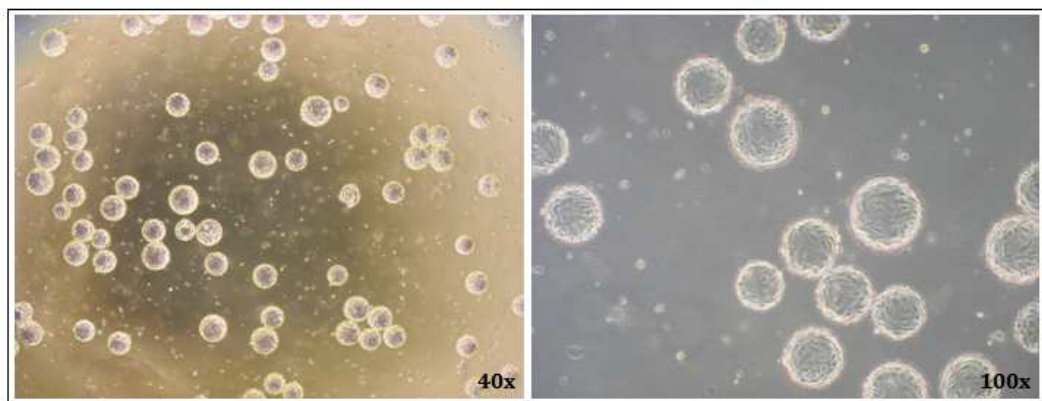


Figure 15: 18h after OECs were added to *Cytodex*TM 1 cellulose beads, they fully adhered and formed monolayers. Those beads were casted later on into fibrin.

In **Figure 16** representative fluorescence images of the investigated coculture systems OECs together with undifferentiated ASCs, adipogenically differentiated ASCs and osteogenically differentiated ASCs as well as OECs in monoculture in fibrin as negative control are illustrated. The cells were labeled with FITC conjugated CD31 antibody and Alexa Fluor® 594 conjugated α -SMA. There is a significant difference between the rudimental, tubular structures generated by OECs in monoculture and the distinct tubules build by OECs in coculture with any of the tested cell types. In the clots containing the cocultures “OECs – Osteogenically differentiated ASCs” and “OECs – Adipogenically differentiated ASCs”, significantly more ASCs are not participating in vessel formation than in the coculture “OECs – Undifferentiated ASCs”, that can be seen on the images showing the α -SMA label.

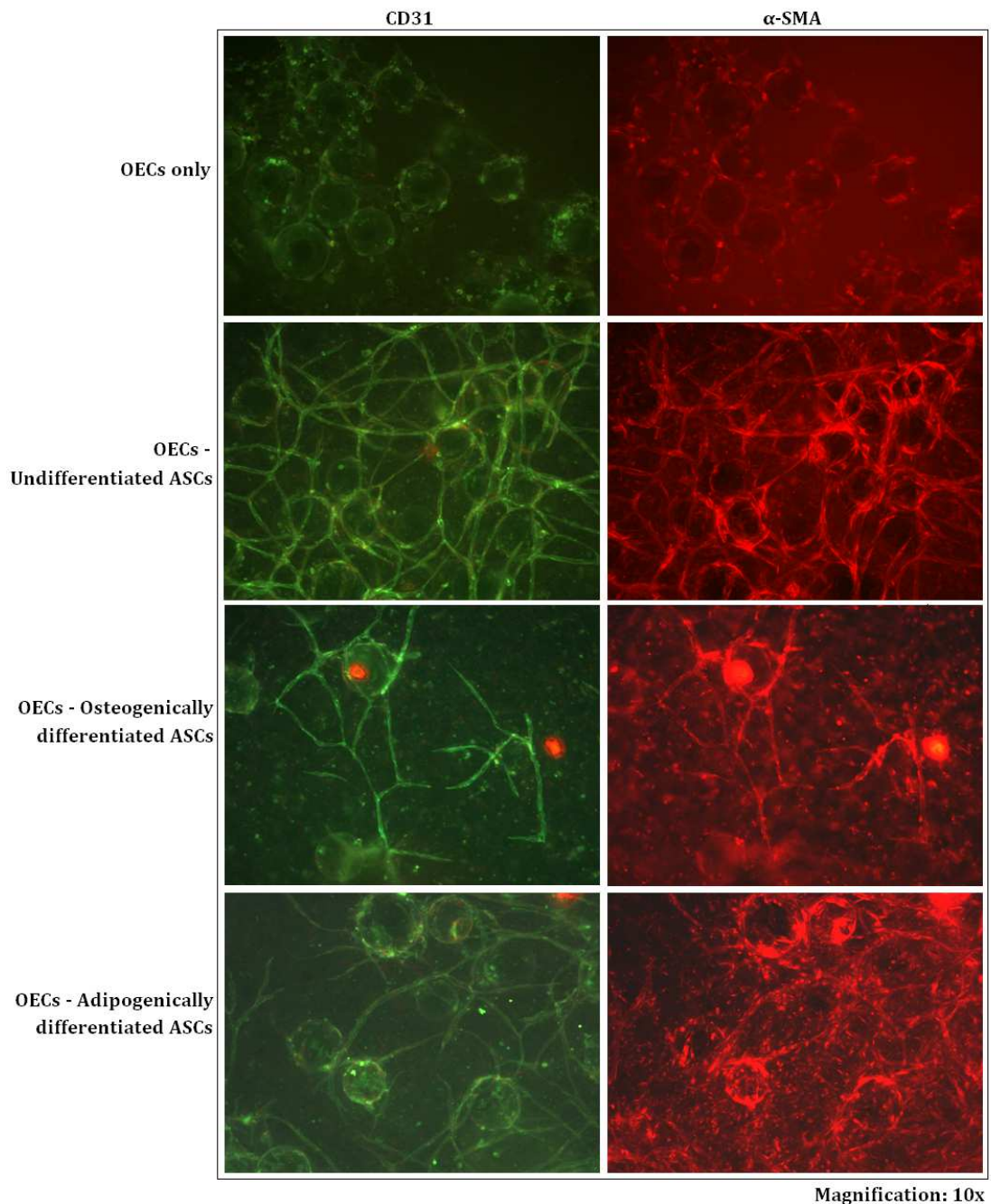


Figure 16: Fluorescence images of OECs on *Cytodex*TM1 cellulose beads in fibrin in monoculture compared to cocultures with undifferentiated, osteogenically differentiated and adipogenically differentiated ASCs at a constant OEC:ASC ratio of 3.5 : 1. In monoculture, OECs did not form distinct tubules but rather lumens around the cellulose beads. The highest anastomosed tubule network was formed by OECs cocultured with undifferentiated ASCs. Less tubules were generated in the OEC – Adipogenically differentiated ASC coculture system while the fewest microvascular structures were generated by OECs cultured together with osteogenically differentiated ASCs. However, in the according image above, the merging of two growing tubules can nicely be seen. Regarding the α-SMA labeling, it appears as if the bulk of ASCs differentiated into the osteogenic as well as into the adipogenic lineage does not contribute to vessel formation compared to the undifferentiated ASCs, where no single cells have been stained by α-SMA.

The quantitative data, which were obtained from three manual countings, are plotted in **Figure 17**. The standard deviation bars result from the three different data sets.

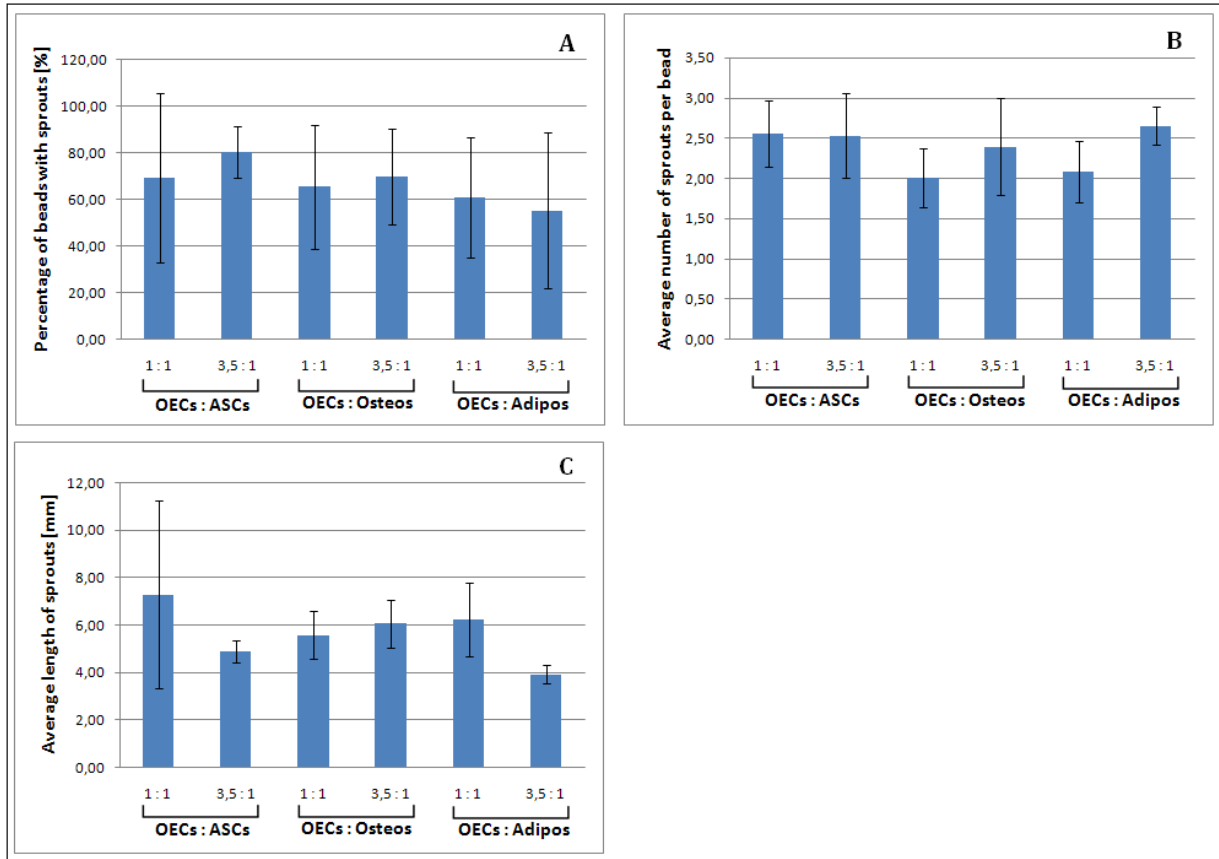


Figure 17: Quantitative analysis of the tubular networks generated by different coculture systems with *Cytodex*TM 1 cellulose beads and different coculture ratios via three parameters. A) The highest percentage of beads from which sprouts arise is 80% in the OEC-ASC coculture system at a ratio of 3.5:1; significantly fewer beads with sprouts were counted in the OEC-Osteo and the OEC-Adipo coculture system at the same ratios, namely 70% and 55%, respectively. **B)** The average number of sprouts per bead was the same for both coculture ratios in the OEC-ASC systems, namely 2.55. This parameter was significantly lower in the OEC-Osteo and the OEC-Adipo 1:1 coculture ratios, namely 2.00 and 2.07, respectively. **C)** The average length of sprouts was the highest in the 1:1 OEC-ASC coculture system with approximately 7.2 mm; it was comparably low in the 1:3.5 OEC-ASC coculture system.

6.4.2 Assembly of the Tubular Structures

Generally, the fluorescence labels against CD31 and α -SMA are both highly specific but at a 10 fold magnification (**Figure 18**), it can hardly be determined whether both antibodies stain the same cells or not. The digital overlay of fluorescence signals arising from Alexa Fluor® 594 nm goat anti-mouse conjugated α -SMA antibody, DAPI and FITC conjugated CD31-antibody at a higher magnification is shown in **Figure 18**. It can be seen, that the endothelial cells, to which intercellular junctions the CD31 antibody binds, form the inner core of the tubules while the α -SMA expressing cells envelope the tubules.

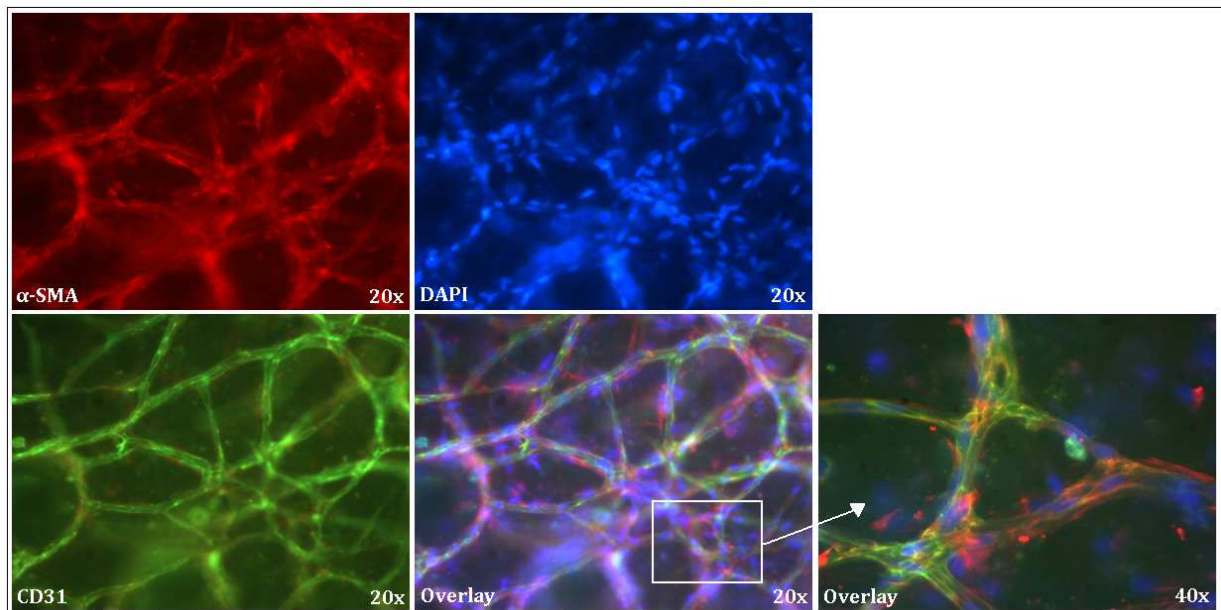


Figure 18: Digital overlay of fluorescence signals of anti- α -SMA antibody, DAPI and anti-CD31 antibody on OECs on beads cocultured with undifferentiated ASCs in a fibrin clot at a ratio of 3.5:1. The identical area of the fibrin clot was illuminated at different UV wavelength and the fluorescence images were overlaid. The overlay proves that the endothelial cells, to which intercellular junctions the CD31 antibody binds, form the inner layer and the α -SMA expressing cells build the outer layer of the generated tubules.

6.4.3 Staining the Tubular Structures against MMP14 and MMP15

As can be seen in **Figure 19A and B**, the OECs building the microvascular networks during coculture with undifferentiated ASCs are positive for MMP14. Due to high unspecific background fluorescence it cannot be definitely ascertained, but there might be also for MMP15 a slight specific staining.

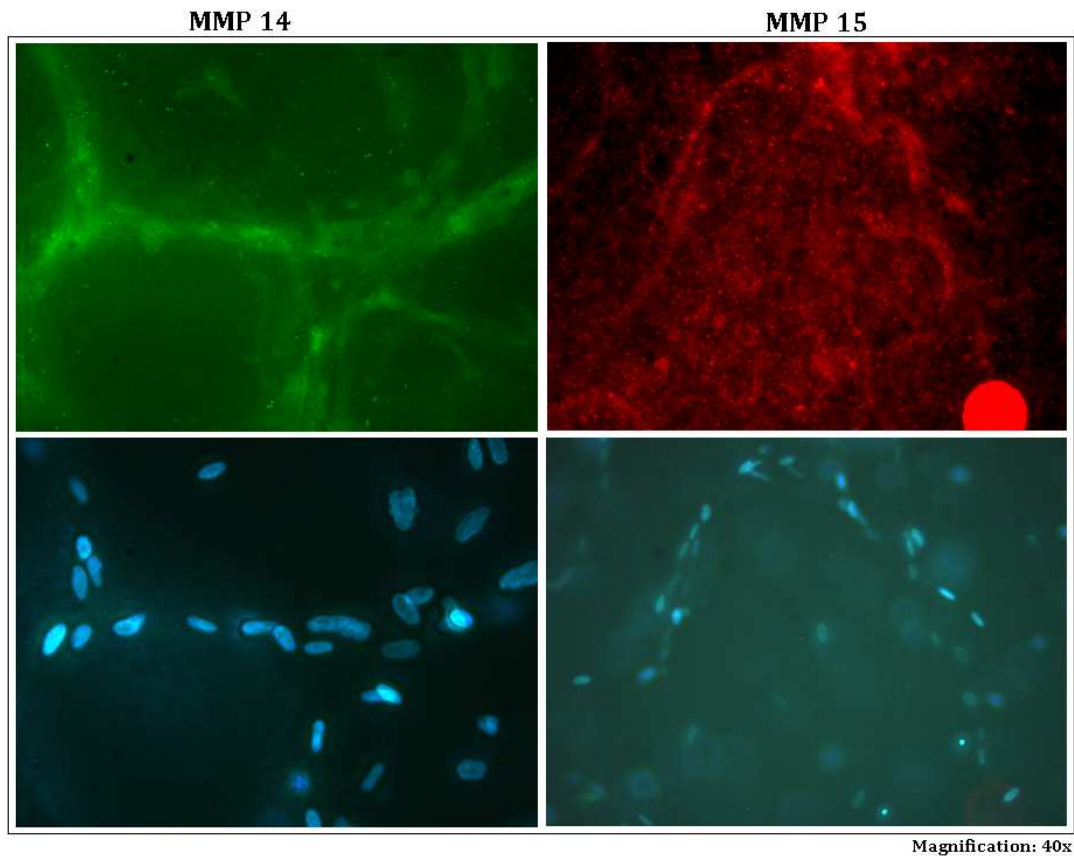


Figure 19: OECs on beads cocultured with undifferentiated ASCs in fibrin clots at a ratio of 1:1 with labeled MMP14 and MMP15. Both proteins appear to be specifically expressed by vascularizing cells.

6.5 Development of microvascular tubules over time

The vertically ordered photo series obtained via the light microscope and depicted in **Figure 20**, show how the microtubules develop over time. The upper image row shows the cells on the first day after they were casted into fibrin. Already there, a few sprouts can be determined in each condition. The images of the middle row show the fibrin clots after one week of culture except for the OECs cocultured with undifferentiated ASCs, which shows the cells two weeks after casting. In the three coculture conditions, it can be seen, how lumen structures are formed. OECs in monoculture digested fibrin and formed a monolayer on the well bottom beneath, although they were actually cultured with the trypsin inhibitor aprotinin. The lower row depicts the coculture systems and the monoculture control systems after three weeks of maintenance. As can be seen, tubule-

like structures have developed from the lumens in each coculture condition while the OECs in the control monoculture further digested the fibrin.

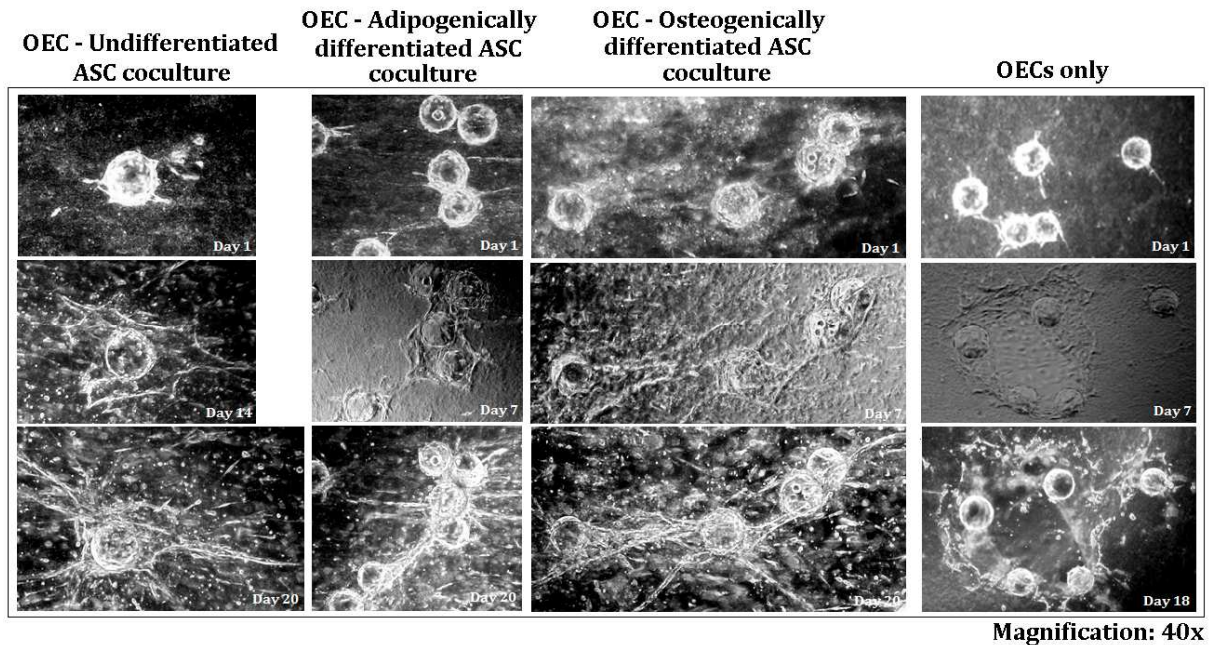
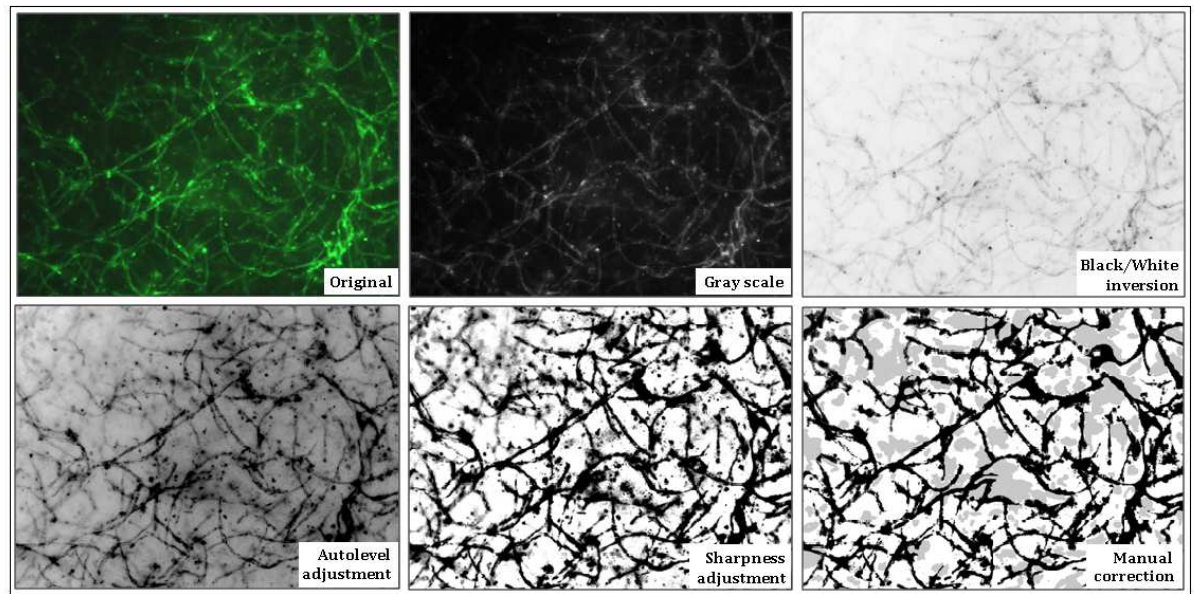


Figure 20: Photo series of the temporal development of tubular structures in fibrin in different OEC-ASC coculture systems compared to OECs in monoculture, documented over three weeks. The upper image row shows the fibrin clots one day after casting; already there, first sprouts could be determined. The mid row illustrates images taken one week after casting, except the very left one of OECs cocultured with undifferentiated ASCs, which was taken two weeks after casting; at those time points, the cells have formed lumens which could hardly be recognized as tubule-like structures. The lower image row finally shows the coculture system after 20 days of incubation, where already cognizable tubular structures have developed. In contrast to the coculture systems, the OECs in monoculture, which can be seen in the image series of the very right column, did not form any tubules but rather digested the fibrin, even though they were cultured in protease inhibitor supplemented medium.

6.5.1 Investigation of different OEC:ASC Coculture Ratios and the Tubular Network Formation with and without *Cytodex*TM 1 Cellulose Beads

Since beads are not feasible for translational purposes, OEC : ASC coculture systems in fibrin without beads were investigated. Prior to the analysis of the microtubular networks, the fluorescence images of the anti-CD31 staining were converted into grey scale images and background noise was reduced using PSE9 as described in **Figure 21**.



Magnification: 20x

Figure 21: Actions taken to convert the original fluorescence images of microtubular networks into standardized gray-scale images, that depict all tubular structures equally intense independent of their original fluorescence intensity.

Figure 22 illustrates the steps, taken for the analysis with *AngioSys*TM. Owing to the precedent, extensive standardization procedure, see **Figure 21**, both, the upper and the lower thresholds can be adjusted to their limits, since the networks are depicted by only black pixels. As can be seen on the left image of **Figure 22**, only the tubular structures are selected after tresholding. The right image shows, how *AngioSys*TM skeletonizes the tubules. The skeleton is depicted by the red lines. The blue crosses represent putative junctions.

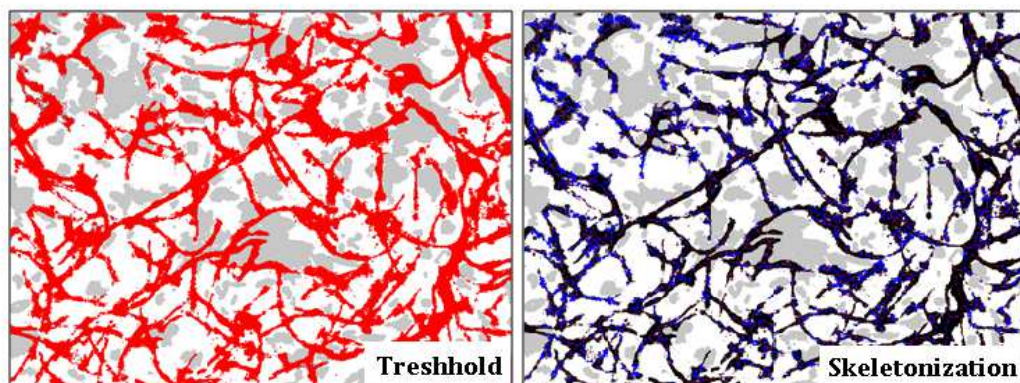


Figure 22: *AngioSys*TM analysis of standardized fluorescence images.

Since the coculture of OECs together with undifferentiated ASCs yielded the highest anastomosed tubular networks, this coculture system was closer investigated. Besides different coculture ratios, the difference between the networks that formed when OECs were seeded onto *Cytodex*TM 1 cellulose beads prior to fibrin clot casting and those formed, when they were added to fibrin as single cell suspension was investigated. **Figure 23** shows standardized fluorescence images of the networks generated in fibrin clots without beads. As expected, the tubules formed by OECs in monoculture are significantly less in number and anastomoses than those arising from OEC-ASC cocultures. The variances between the different coculture ratios are determined quantitatively by *AngioSys*TM analysis (**Figure 25**).

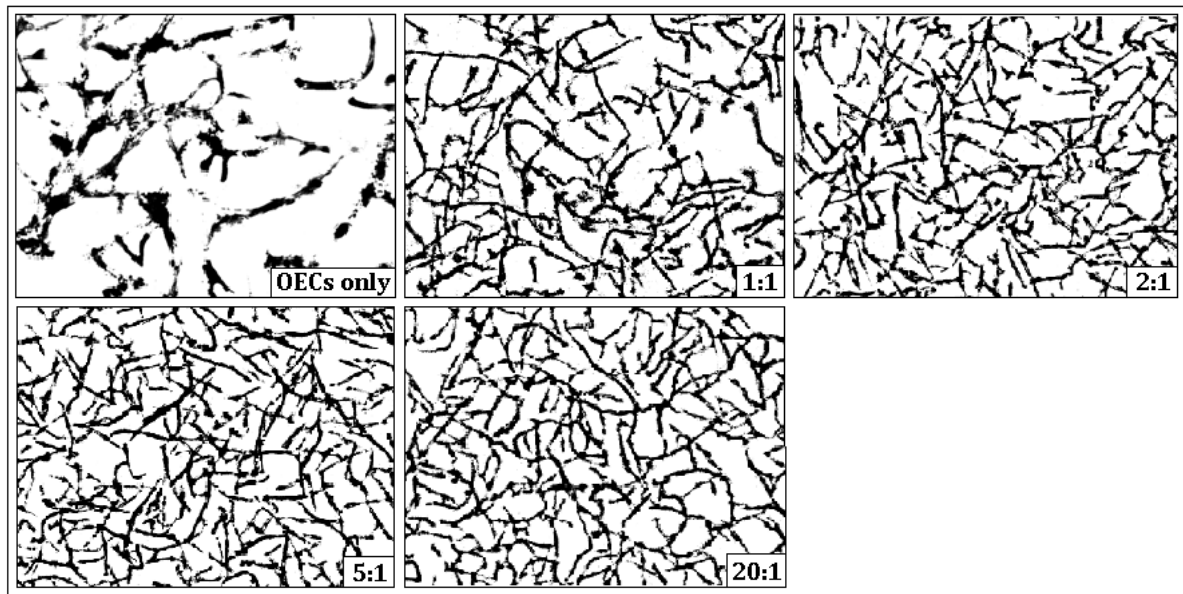


Figure 23: Standardized fluorescence images of fibrin clots without *Cytodex*TM 1 cellulose beads, in which OECs were monocultured or cocultured together with undifferentiated ASCs at ratios of 1:1, 2:1, 5:1 and 20:1.

Figure 24 depicts standardized fluorescence images of the microtubular networks formed in fibrin clots, in which OECs on *Cytodex*TM 1 beads were cocultured together with undifferentiated ASCs. Again, the microtubular network formed in the OEC monoculture control was disproportionately less anastomosed than those formed during the OEC-ASC cocultures.

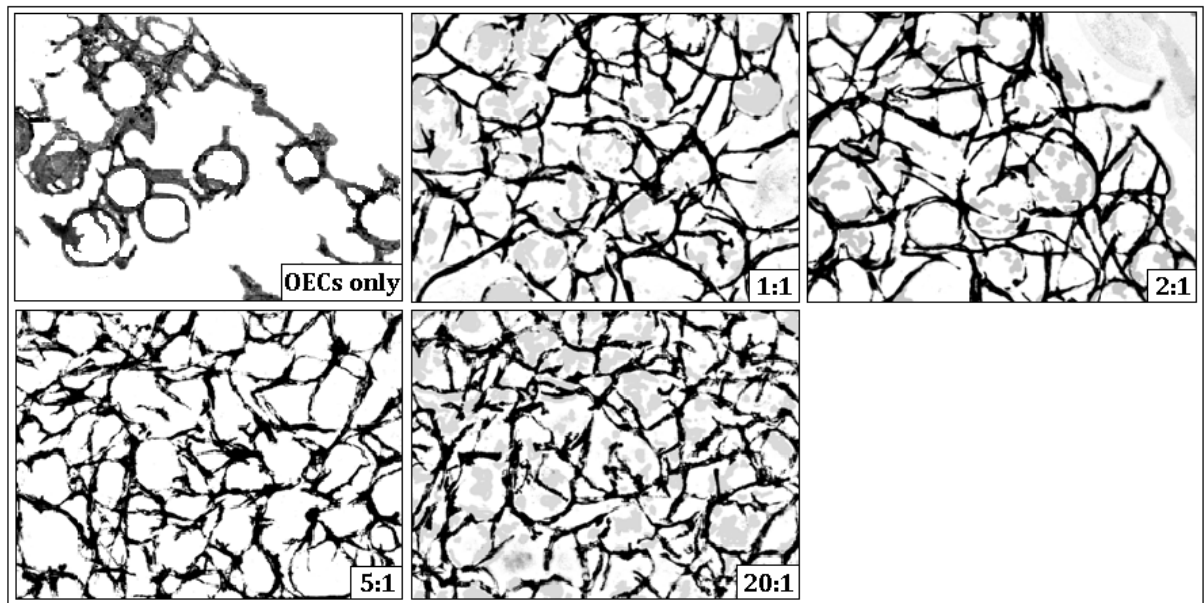


Figure 24: Standardized fluorescence images of fibrin clots, in which OECs on *Cytodex*TM 1 cellulose beads were monocultured or cocultured together with undifferentiated ASCs at ratios of 1:1, 2:1, 5:1 and 20:1.

The quantitative results of the standardized analysis of the microtubular networks generated in fibrin clots with and without cellulose beads at different coculture ratios are plotted in **Figure 25**. The standard deviation bars arise from the analysis of three different images of each condition.

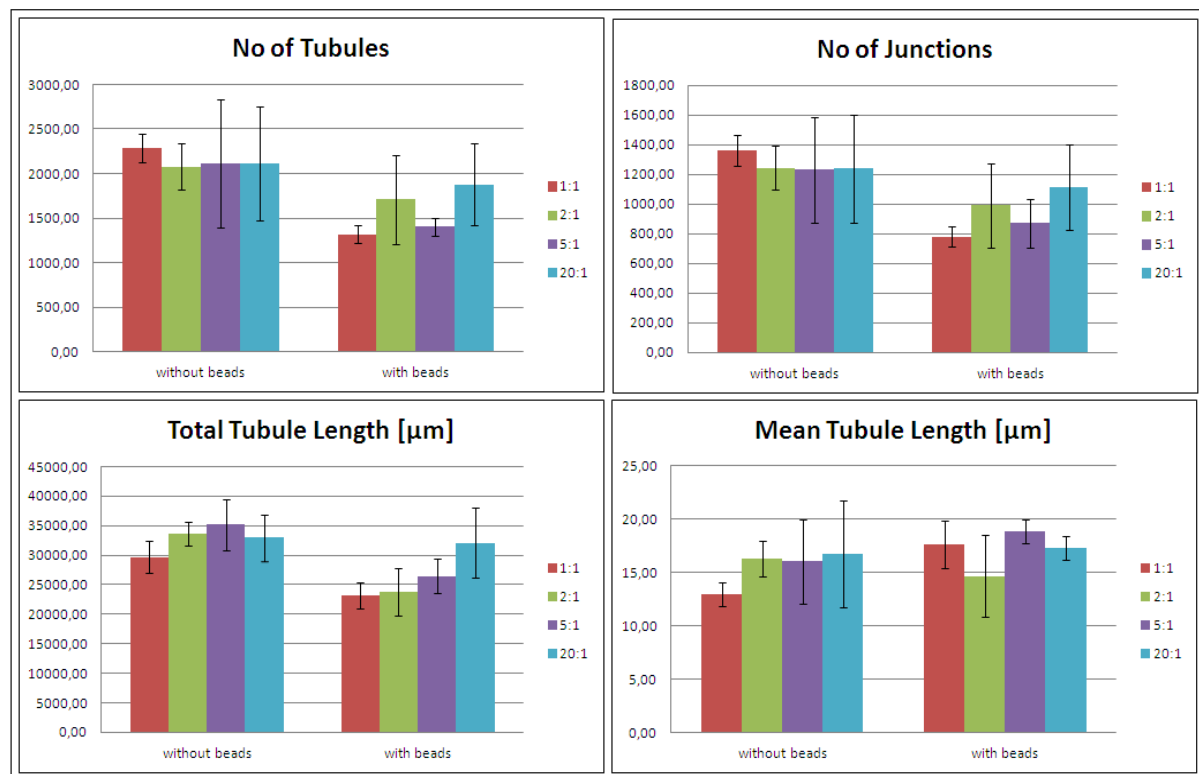


Figure 25: Data of standardized analysis by *AngioSys*TM of fluorescence images of microtubular networks in fibrin clots with and without beads at different OEC:ASC coculture ratios. OEC monoculture controls were not included in the *AngioSys*TM analysis due to the apparent non-linearity determined on the epifluorescence microscopical photos. Comparing the coculture systems with and without beads, the number of tubules as well as the number of junctions is higher in the first than in the second, regardless of the coculture ratio. Also the total tubule length was generally higher in the clots without beads compared to that of the clots with beads. Although the total tubule length is generally higher in the clots without beads, the mean tubule length is lower; this denotes that the degree of anastomosis in clots without beads is higher than that of the clots with beads.

6.1 Placental Decellularization

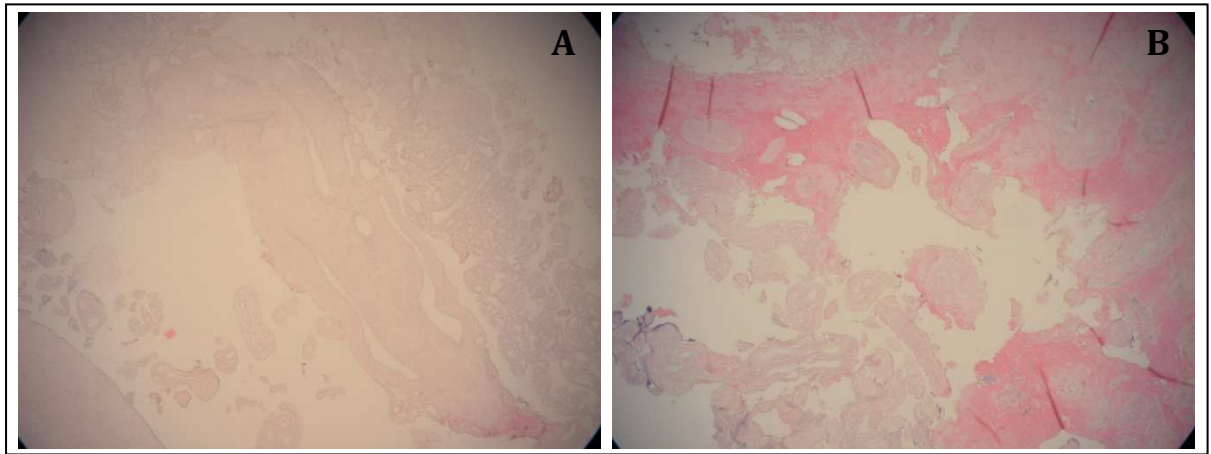
It has been shown, that microvascular structures can be generated *in vitro* by co-culturing outgrowth endothelial cells together with adipose derived stem cells in fibrin matrix. However, only small vessel-like structures with circumferences built from at most 4 cells could be produced. To achieve larger vessels, it was taken into consideration to seed both cell types, OECs and ASCs, into decellularized placental tissue. Due to a limitation in time for this thesis, only the tissue decellularization could be finished, while the cell behavior in the matrix could not be investigated any more.

Figure 26 shows the placental tissue piece after 13 days of decellularization. The brown substance at the interface between the permanent venous catheter and the tissue is solidified glue, which had to be applied on Day 3 of decellularization, since one of the vessels was penetrated accidentally with a catheter.



Figure 26: Placental tissue after 13 days of decellularization. The tubes are connected to the tissue via permanent venous catheters. The brown color arises from self-mixed glue, which was applied to a leakage after accidental penetration.

Microtome-cut, in paraffin casted cross sections of a non-treated and a treated vessel after H&E staining are depicted in **Figure 27**. On the images, it can be seen, that the untreated vessel is lined by blue-appearing cell nuclei, while no cell nuclei can be determined in the decellularized vessel.



Magnification: 4x

Figure 27: H&E stained placental tissue; A) not decellularized vessel. B) decellularized vessel. The nuclei of cells are colored blue by hemalum. On the left image, the vessel walls are lined by cells, which appear blue due to the hematoxylin staining while no cells can be seen on the left image. However, the decellularized vessel appears destroyed which is probably due to the mechanical stress to which it was encountered for the previous 13 days.

7. DISCUSSION AND CONCLUSION

7.1 Outgrowth Endothelial Cell Isolation and Characterization of OECs and ASCs by Flow Cytometry

The isolation of primary outgrowth endothelial cells from human peripheral blood was probably the most critical undertaking of this study. From 9 platings, only 2 isolated cell populations could be used for microvascularization experiments. However, in almost all attempts, cells exhibiting cobblestone-like morphology adhered to the cell culture plate surface after 10 to 20 days of culture. The two successful isolations, on the other hand, were growing rapidly until approximately p8. Those cells expanded to 80% confluence within 2-3 days after splitting them at a ratio of 1:2 or sometimes even 1:3.

7.2 Differentiation into the Adipogenic and Osteogenic Lineage

As can be seen in **Figure 10**, the adipogenic and osteogenic differentiation were both successful. The use of differentiated ASCs was critically reconsidered after it was found that the cells were still capable to differentiate into the osteogenic lineage when they were already differentiated adipogenically and *vice versa* (**Figure 14**). Since “trans-differentiation” has been mentioned in the literature only in connection to embryonic development [Jain *et al.*, 2003], it can be suggested that not adipogenically or osteogenically differentiated ASCs differentiated into the other lineage, respectively, but that rather still undifferentiated ASCs residing among the differentiating ones have to be responsible for that event. The adipogenically differentiated ASCs could get lost during centrifugation after detachment from the original culture vessel due to their intracellular vacuolar oil content which made them flood in the aqueous cell culture medium. Another hypothesis is that the intracellular oil-containing vacuoles burst upon the mechanical stress applied to the cells during detachment and centrifugation, which led to cell death.

The osteogenically differentiated ASCs on the other hand could hardly be detached from the cell culture plate due to the secreted, mineralized nodules. They might not survive the mechanical scraping off in contrast to the still undifferentiated ASCs, which could easily be detached anyway. This hypothesis would be backed up by the fact, that most tubules were generated when OECs were cocultured with originally undifferentiated ASCs, since there were most viable ASCs supporting the vessel formation.

7.3 Coculture of OECs and ASCs in Fibrin

7.3.1 Coculture of OECs with Undifferentiated ASCs, Osteogenically and Adipogenically Differentiated ASCs compared to OEC Monoculture in Fibrin

Due to the fact, that almost no living osteogenically or adipogenically differentiated ASCs could be transferred into fibrin, they are not taken into consideration for supporting microvascular tubule formation anymore. However, besides the significant difference between OEC monoculture and the coculture systems, it can be seen in **Figure 16**, that the number of ASCs is a critical parameter for the formation of tubules. Compared to the network generated by coculture of OECs together with undifferentiated ASCs, the other two conditions, coculture with “adipogenically differentiated” and “osteogenically differentiated” ASCs, resulted in less tubules, since much less ASCs were present there. The enhancement of tube formation by cell cocultivation has been previously shown by, for instance, Black *et al.* who reported capillary tube formation upon coculture of keratinocytes, dermal fibroblasts, and HUVECs while no vessels were generated in the monoculture of each cell type [Black *et al.*, 1998]. Also Borges *et al.* showed that ECs proliferated when cocultured with preadipocytes in fibrin while they underwent apoptosis in monoculture [Borges *et al.*, 2007]. However, the positive effect of an increasing number of OECs at a constant number of ASCs or any other cocultured cell type has not been mentioned in the literature until now. Nevertheless, from the diagrams of **Figure 17**, it can be concluded that with an increasing number of OECs present in fibrin, the percentage of beads with sprouts and the number of sprouts per bead also increases.

The average length of sprouts is inversely proportional to the number of OECs, which results from the fact, that more tubular junctions are established.

7.3.2 Assembly of the Tubular Structures

It has been shown already in 1998 by Hirschi *et al.*, that embryonic stem cells (ESCs) upregulated the expression of three smooth muscle cell specific markers and changed their shape from polygonal to spindle-shaped upon under-agarose coculture with endothelial cells, while none of these events occurred in monoculture of the embryonic stem cells [Hirschi *et al.*, 1998]. Using neutralizing antibodies, it was demonstrated, that PDGF-B is essential for ESC recruitment in contrast to PDGF-A and bFGF. Nehls *et al.* even observed the phenomenon, that vascular smooth muscle cells (expression of α -SMA) spatially arranged themselves to capillary like networks in monoculture in a fibrin matrix. This indicates that cells co-cultured with endothelial cells might actively contribute to vessel generation [Nehls *et al.*, 1994].

The cells generating the microvascular networks in this study were also positive for α -SMA, as can be seen in **Figure 18**. Digital overlays of the signals arising from anti-CD31 and anti- α -SMA antibody-antigen complexes reveal that the tubules are built from endothelial cells enveloped by α -SMA expressing cells, which is depicted on the left image of **Figure 18** at a 40x magnification. This alignment suggests that ASCs interact as stabilizing mural cells with the vascularizing OECs. The expression of α -SMA has also been demonstrated in cocultures of HUVECs with ASCs in fibrin [Verseijden *et al.*, 2012].

Due to the specifically important role of the expression of matrix metalloproteinases MMP14 (MT1-MMP) and MMP15 by vascularizing endothelial cells [Yana *et al.*, 2007; Davis *et al.*, 2002; van Hinsbergh *et al.*, 2008], the microvessel-like structures generated in this study were stained against these. As can be seen in **Figure 19**, the cells establishing the microvessels express both, MMP14 and MMP15.

7.4 Investigation of different OEC:ASC coculture ratios and the tubular network formation with and without *Cytodex*TM 1 cellulose beads

The standardization procedure, depicted in **Figure 21** was applied to all obtained fluorescence images of the tubular networks to ensure realistic evaluation by *AngioSys*TM. However, the manual deletion of fluorescence signals that do not arise from tubular structures, but for instance from single cells or the background brings in a potential error source. If those deletions were not conducted, *AngioSys*TM would not give any realistic data later on, since there is no pattern recognition function or something similar integrated. However, the original fluorescence image was constantly used as reference during the correction actions to ensure, that no tubule-like structures were accidentally removed.

Owing to the precedent, extensive standardization, both, the upper and the lower thresholds could be adjusted to their limits, since the networks were depicted by only black pixels. As can be seen on the left image of **Figure 22**, only the tubular structures were selected after thresholding. The right image shows, how *AngioSys*TM skeletonizes the tubules. The skeleton is depicted by the red lines. As can be seen, the software, indeed, mostly recognizes tubules despite irregularities. The blue crosses represent putative junctions, though there are far less real junctions. Therefore, the number of junctions cannot be taken as a meaningful parameter.

The data of **Figure 25** clearly suggest that all microvascular networks generated in fibrin without *Cytodex*TM 1 cellulose beads resulted in higher numbers of tubules, higher total tubule lengths and lower mean tubule lengths. The last mentioned parameter indicates a higher degree of anastomosis. The diagrams generally show the same as those of **Figure 17**, because the number of OECs in clots with beads is approximately 2×10^4 (Eq. 7) while it is approximately 2×10^5 in the clots without beads, thus 10 times higher.

To achieve a cell number of 2×10^5 on beads, this would require 2000 beads. Looking at the used bead density of 200 beads per clot, this would mean a 10 fold increase, which would further mean, that less free space would be available in the fibrin for tubule

formation. Taking this into account, it might be advisable to focus all further research activities onto vascularization without *Cytodex*TM 1 cellulose beads, since higher cell numbers can be achieved. Moreover, concerning potential clinical application, the risk of rejection after implantation of the fibrin clots decreases substantially without the non-biodegradable cellulose beads.

Inspecting the detailed data of the fibrin clots without beads of **Figure 25**, it can be suggested, that the OEC-ASC coculture ratios 5:1 and 20:1 resulted in the networks composed of most tubules and the highest total tubule length. Since there are only minor differences between those two conditions, it might be advisable to stay with the optimal coculture ratio of 5:1, since four times more OECs (20:1) did not result in any advantageous effects any more. The above considerations suggest that the condition resulting in the “best” microvascular network is the coculture of OECs together with ASCs at a ratio of 5:1 without previously seeding the OECs onto *Cytodex*TM 1.

7.5 Placental decellularization

The approach of generating macroscopic vascular systems by seeding autologous OECs into an autologous tissue appears highly promising. The decellularization of placental tissue conducted during this study was successful, which was confirmed by H&E staining of a microtome-cut paraffin slice. In comparison to that, an untreated vessel of the same tissue piece was still aligned by cells.

Unfortunately, it could not be further investigated, whether it was possible to seed OECs into this decellularized tissue piece and how they would behave in there due to a lack in time.

7.6 Conclusion and Outlook

In this study, it was shown, that *in vitro* coculture of peripheral blood derived OECs and ASCs, obtained from liposuction material, in fibrin matrices results in stable microvascular networks, while the cells did not form stable tubular structures in monoculture. By generating microvascular networks *in vitro*, it will soon be possible to regenerate autologous vascularized tissue and thus treat for instance myocardial or critical limb ischemia [Schächinger *et al.* 2004, Kawamura *et al.* 2005]. Until now, research was mainly focused on HUVECs but it has recently been shown, that OECs have a comparable angiogenic potential [Finkenzeller *et al.*, 2007]. From a clinical point of view the usage of OECs is more favorable than HUVECs, because they are an autologous cell source and can be obtained from adults either from the blood or bone marrow by a minimal invasive biopsy. ASCs are abundant multipotent stem cells which can be easily isolated from e.g. human subcutaneous lipoaspirates [Dubois *et al.*, 2008].

Hereafter, the stability of the generated microvascular networks as well as their ability to anastomose with pre-existing capillaries has to be tested *in vivo*. All shown results were obtained by ASC/OEC cocultivation in fibrin at a concentration of 2.5 mg/ml, which most probably is not solid enough for subcutaneous implantation. Thus, network formation should be further investigated at higher fibrin concentrations.

8. LITERATURE

- Abe T**, Okamura K, Ono M, and Kohno O. Induction of vascular endothelial tubular morphogenesis by human glioma cells. A model system for tumor angiogenesis. *J Clin Invest* 92(1): 54-61, 1993
- Ahrens I**, Domeij H, Topcic D, Haviv I, Merivirta RM, Agrotis A, Leitner E, Jowett JB, Bode C, Lappas M, and Peter K. Successful *in vitro* expansion and differentiation of cord blood derived CD34+ cells into early endothelial progenitor cells reveals highly differential gene expression. *PLoS One*. 6(8), e23210. Epub 2011
- Allen P**, Melero-Martin J, Bischoff J. Type I collagen, fibrin and PuraMarix matrices provide permissive environments for human endothelial and mesenchymal progenitor cells to form neovascular networks. *J Tissue Eng Regen Med* 5(4): e74-86, 2011
- Amini AR**, Laurencin CT, and Nukavarapu SP. Differential analysis of peripheral blood- and bone marrow-derived endothelial progenitor cells for enhanced vascularization in bone tissue engineering. *J Orthop Res* 30 (9): 1507-17, 2012
- Arnaoutova I**, George J, Kleinman HK, Benton G. Basement Membrane Matrix (BME) has multiple uses with stem cells. *Stem Cell Rev* 128 (8): 163-9, 2012
- Arao T**, Matsumoto K, Furuta K, Kudo K, Kaneda H, Nagai T, Sakai K, Fujita Y, Tamura D, Aomatsu K, Koizumi F, Nishio K. Acquired drug resistance to vascular endothelial growth factor receptor 2 tyrosine kinase inhibitor in human vascular endothelial cells. *Anticancer Res* 31(9): 2787-96, 2011
- Asahara T**, Masuda H, Takahashi T, Kalka C, Pastore C, Silver M, Kearne M, Magner M, and Isner JM. Bone marrow origin of endothelial progenitor cells responsible for postnatal vasculogenesis in physiological and pathological neovascularization. *Circ Res* 85: 221, 1999
- Baker JR**. Experiments on the action of mordants; 2. Aluminium-haematein. *J Micr Sci* 103 (4): 493-517, 1962
- Barsotti MC**, Felice F, Balbarini A, and Di Stefano R. Fibrin as a scaffold for cardiac tissue regeneration. *Biotechnol Appl Biochem* 58 (5): 301-10, 2011
- Baudis S**, Steyrer B, Pulka T, Wilhelm H, Weigel G, Bergmeister H, Stampfl J, and Liska R. Photopolymerizable elastomers for vascular tissue regeneration. *Macromolecular Symposia* 296 (1): 121-6, 2010
- Baudis S**, Nehl F, Ligon SC, Nigisch A, Bermeister H, Bernhard D, Stampfl J, and Liska R. Elastomeric degradable biomaterials by photopolymerization-based CAD-CAM for vascular tissue engineering. *Biomed Mater* 6 (5): 055003, Epub 2011
- Bayless KJ**, Salazar R, and Davis GE. RGD-dependent vacuolation and lumen formation observed during endothelial cell morphogenesis in three-dimensional fibrin matrices involves the $\alpha(v)\beta(3)$ and $\alpha(5)\beta(1)$ integrins. *Am J Pathol* 156: 1673, 2000
- Black AF**, Berthod F, L'heureux N, Germain L, and Auger FA. *In vitro* reconstruction of human capillary-like network in a tissue engineered skin equivalent. *FASEB J* 12: 1331, 1998
- Black AF**, Hudon V, Damour O, Germain L, and Auger FA. A novel approach for studying angiogenesis: a human skin equivalent with a capillary-like network. *Cell Biol Toxicol* 2: 81-90, 1999
- Blum Y**, Belting HG, Ellertsdottir E, Herwig L, Luders F, and Affolter M. Complex cell rearrangements during intersegmental vessel sprouting and vessel fusion in the zebrafish embryo. *Dev Biol* 316: 312-22, 2008
- Borges J**, Mueller MC, Padron NT, Tegtmeier F, Lang EM, and Stark GB. Engineered adipose tissue supplied by functional microvessels. *Tissue Eng* 6: 1263-70, 2003
- Borges J**, Muller MC, Momeni A, Stark GB, and Torio-Padron N. *In vitro* analysis of the interactions between preadipocytes and endothelial cells in a 3D fibrin matrix. *J Soc Minim Invasive Ther* 16: 141, 2007
- Böyum A**. Isolation of mononuclear cells and granulocytes from human blood. isolation of mononuclear cells by one centrifugation, and of granulocytes by combining centrifugation and sedimentation at 1 g. *Scand J Clin Lab Invest Suppl* 97: 77-89, 1968
- Carmeliet P**. Mechanisms of angiogenesis and arteriogenesis. *Nat Med* 6: 389-95, 2000
- Carmeliet P, and Conway EM**. Growing better blood vessels. *Nat Biotechnol* 19: 1019, 2001
- Ceylan H**, Tekinay AB, and Guler MO. Selective adhesion and growth of vascular endothelial cells on bioactive peptide nanofiber functionalized stainless steel surface. *Biomaterials* 32 (34): 8797-805, 2011
- Chambers RC**, Leoni P, Kaminski N, Laurent GJ, and Heller RA. Global expression profiling of fibroblast responses to transforming growth factor- $\beta(1)$ reveals the induction of inhibitor of differentiation- and provides evidence of smooth muscle cell phenotypic switching. *Am J Pathol* 162: 533-46, 2003

- Corada M.**, Zanetta L., Orsenigo F., Breviario F., Lampugnani M.G., Bernasconi S., Liao F., Hicklin D.J., Bohlen P., Dejana E. A monoclonal antibody to vascular endothelial-cadherin inhibits tumor angiogenesis without side effects on endothelial permeability. *Blood* 100 (3): 905–11, 2002
- Corbeil D**, Röper K, Hellwig A, Tavian M, Miraglia S, Watt SM, Simmons PJ, Peault B, Buck DW, and Huttner HB. The human AC133 hematopoietic stem cell antigen is also expressed in epithelial cells and targeted to plasma membrane protrusions. *J Biol Chem* 275 (8): 5512–20, 2000
- Davis GE**, Bayless KJ, and Mavila A. Molecular basis of endothelial cell morphogenesis in three-dimensional extracellular matrices. *Anatom Record* 268: 252–275, 2002
- Davis GE**, Koh W, and Stratman AN. Mechanisms controlling human endothelial lumen formation and tube assembly in three-dimensional extracellular matrices. *Birth Defects Res C Embryo Today* 81: 270, 2007.
- Deponti D**, Di Giancamillo A, Mangiavini L, Pozzi A, Frascini G, Sosio C, Domeneghini C, and Peretti GM. Fibrin based model for cartilage regeneration: tissue maturation from *in vitro* to *in vivo*. *Tissue Eng Part A* 18 (11-12): 1109-1122, 2012
- De Smet F**, Inmaculada S, De Bock K, Hohenesinner PJ, and Carmeliet P. Mechanisms of vessel branching – Filopodia on Endothelial Tip cells lead the way. *Arterioscler Thromb Vasc Biol* 29: 639-49, 2009
- Ding R**, Darland DC, Parmacek MS, and D’Amore PA. Endothelial-mesenchymal interactions *in vitro* reveal molecular mechanisms of smooth muscle/pericyte differentiation. *Stem Cells Dev* 13: 509, 2004
- Di Matteo P**, Arrigoni GL, Alberici L, Corti A, Gallo-Stampino C, Traversari C, Doglioni C, and Rizzardi GP. Enhanced expression of CD13 in vessels of inflammatory and neoplastic tissues. *J Histochem Cytochem* 59(1): 47-59, 2011
- Doi K**, Soga Y, Iwakura A, Ueyama K, Yamahara K, Itoh H, Nishimura K, Tabata Y, and Komeda M. Enhanced angiogenesis by gelatin hydrogels incorporating basic fibroblast growth factor in rabbit model of hind limb ischemia. *Heart Vessels* 22: 104, 2007
- Dubois SG**, Zvonick S, Kilroy G, Wu X, Carling S, Halvorsen YD, Ravussin E, Gimble JM. Isolation of human adipose derived stem cells from biopsies and liposuction specimens. *Methods Mol Biol* 449: 69-79, 2008
- Elenbaas B and Weinberg RA**. Heterotypic signaling between epithelial tumor cells and fibroblasts in carcinoma formation. *Exp Cell Res* 264: 169-84, 2001
- Finkenzeller G**, Torio-Patron N, Momeni A, Mehlhorn AT, Stark GB. *In vitro* angiogenesis properties of endothelial progenitor cells: a promising tool for vascularization of ex vivo engineered tissues. *Tissue Eng* 13: 1413-20, 2007
- Fuchs S**, Ghanaati S, Orth C. Contribution of outgrowth endothelial cells from human peripheral blood on *in vivo* vascularization of bone tissue engineered constructs based on starch polycaprolactone scaffolds. *Biomaterials* 30: 526-34, 2009
- Fuchs S**, Hermanns MI, Kirkpatrick CJ. Retention of a differentiated endothelial phenotype by outgrowth endothelial cells isolated from human peripheral blood and expanded in long-term cultures. *Cell Tissue Res* 326: 79-92, 2006
- Gray H**. Anatomy of the human body. 1918
- Gohongi T**, Fukumura D, Boucher Y, Yun CO, Soff GA, Compton C, Todoroki T, Jain RK. Tumor-host interactions in the gallbladder suppress distal angiogenesis and tumor growth: involvement of transforming growth factor β 1. *Nat Med* 5: 1203-8, 1999
- Gu A**, Shively JE. Angiopoietins-1 and -2 play opposing roles in endothelial sprouting of embryoid bodies in 3D culture and their receptor Tie-2 associates with the cell-cell adhesion molecule PECAM1. *Exp Cell Res* 317(15): 2171-82, 2011
- Hedrich HC**, Simunek M, Reisinger S, Ferguson J, Gulle H, Geppelt A, Redl H. Fibrin chain cross-linking, fibrinolysis, and *in vivo* sealing efficacy of differently structured fibrin sealants. *J Biomed Mater Res B Appl Biomater* 100 (6): 1507-12, 2012
- Hellström M**, Gerhardt H, Kalén M, Li X, Eriksson U, Wolburg H, and Betsholtz C. Lack of pericytes leads to endothelial hyperplasia and abnormal vascular morphogenesis. *J Cell Biol* 153: 543-53, 2001
- Hirschi KK**, Rohovsky SA, and D’Amore PA. PDGF, TGF-beta, and heterotypic cell-cell interactions mediate endothelial cell-induced recruitment of 10T1/2 cells and their differentiation to a smooth muscle fate. *J Cell Biol* 141: 805, 1998
- Horn PA**, Tesch H, Staib P, Kube D, Diehl V, and Voliotis D. Expression of AC133, a novel hematopoietic precursor antigen, on acute myeloid leukemia cells. *Blood* 93 (4): 1435–7, 1999
- Hosseinkhani H**, Hosseinkhani M, Khademhosseini A, Kobayashi H, and Tabata Y. Enhanced angiogenesis through controlled release of basic fibroblast growth factor from peptide amphiphile for tissue regeneration. *Biomaterials* 27: 5836, 2006

- Hristov M**, Schmitz S, Schuhmann C, Leyendecker T, von Hundelshausen P, Krötz F, Sohn HY, Nauwelaers FA, and Weber C. An optimized flow cytometry protocol for analysis of angiogenic monocytes and endothelial progenitor cells in peripheral blood. *Cytometry A* 75(10): 848-53, 2009
- Hungerford JE and Little CD**. Developmental biology of the vascular smooth muscle cell: building a multilayered vessel wall. *J Vasc Res* 36: 2-27, 1999
- Ingram DA**, Mead LE, Moore DB, Woodard W, Fenoglio A, and Yoder MC. Vessel wall derived endothelial cells rapidly proliferate because they contain a complete hierarchy of endothelial progenitor cells, *Blood* 105 (7): 2783-6, 2005
- Ispanovic E**, Serio D, and Haas TL. Cdc42 and RhoA have opposing roles in regulating membrane type 1-matrix metalloproteinase localization and matrix metalloproteinase-2 activation. *Am J Physiol Cell Physiol* 295: C600–10, 2008
- Jain RK**. Molecular regulation of vessel maturation. *Nature Medicine* 9 (6): 685-93, 2003
- Kamei M**, Saunders WB, Bayless KJ, Dye L, Davis GE, and Weinstein BM. Endothelial tubes assemble from intracellular vacuoles in vivo. *Nature* 442: 453– 6, 2006
- Kanda N**, Morimoto N, Takemoto S, Ayvazyan AA, Kawai K, Sakamoto Y, Taira T, and Suzuki S. Efficacy of novel collagen/gelatin scaffold with sustained release of basic fibroblast growth factor for dermis-like tissue regeneration. *Ann Plast Surg* 69 (5): 569-74, 2011
- Kaigler D**, Wang Z, Horger K, Mooney DJ, and Krebsbach PH. VEGF scaffolds enhance angiogenesis and bone regeneration in irradiated osseous defects. *J Bone Miner Res* 21: 735, 2006
- Kaully T**, Kaufman-Francis K, Lesman A, and Levenberg S. Vascularization— The conduit to viable engineered tissues. *Tissue Eng B* 15 (2): 159-69, 2009
- Kawamura A**, Horie T, Tsuda I, Ikeda A, Egawa H, Imamura E, Iida J, Sakata H, Tamaki T, Kukita K, Meguro J, Yonekawa M, Kasai M. Prevention of limb amputation in patients with limbs ulcers by autologous peripheral blood mononuclear cell implantation. *Ther Apher Dial* 9 (1): 59-63, 2005
- Kilarski WW**, Samolov B, Petersson L, Kvanta A, and Gerwins P. Biomechanical regulation of blood vessel growth during tissue vascularization. *Nat Med* 15(6): 657-64, 2009
- Kim J**, Rubin N, Huang Y, Tuan TL, and Lien CL. *In vitro* culture of epicardial cells from adult zebra fish heart on a fibrin matrix. *Nat Protoc* 7 (2): 247-55, 2012
- Kitahara T**, Hiromura K, Ikeuchi H, Yamashita S, Kobayashi S, Kuroiwa T, Kaneko Y, Ueki K, and Nojima Y. Mesangial cells stimulate differentiation of endothelial cells to form capillary-like networks in a three-dimensional culture system. *Nephrol Dial Transplant* 20: 42, 2005
- Kluk, MJ** and Jöa T. Signaling of sphingosine-1-phosphate via the S1P/EDG-family of G-protein-coupled receptors. *Biochim Biophys Acta* 1582: 72-80, 2002
- Koike N**, Fukumura D, Gralla O, Au P, Schechner JS, and Jain RK. Tissue engineering: creation of long-lasting blood vessels. *Nature* 428(6979): 138-9, 2004
- Lamallice L**, Houle F, Jourdan G, and Huot J. Phosphorylation of tyrosine 1214 on VEGFR2 is required for VEGF-induced activation of Cdc42 upstream of SAPK2/p38. *Oncogene* 23: 434–45, 2004
- Leach JK**, Kaigler D, Wang Z, Krebsbach PH, and Mooney DJ. Coating of VEGF-releasing scaffolds with bioactive glass for angiogenesis and bone regeneration. *Biomaterials* 27: 3249, 2006.
- Leslie-Barbick JE**, Shen C, Chen C, and West JL. Micron-scale spatially patterned, covalently immobilized vascular endothelial growth factor on hydrogels accelerates endothelial tubulogenesis and increases cellular angiogenic responses. *Tissue Eng Part A* 17 (1-2): 221-9, 2011
- Leong A**, Cooper K, and Leong F J. Manual of Diagnostic Cytology (2 ed.). *Greenwich Medical Media*, 121–4, 2003
- Lin Y**, Weisdorf DJ, Solovey A, and Hebbel RP. Origins of circulating endothelial cells and endothelial outgrowth from blood. *J Clin Invest* 105(1): 71-7, 2000
- Loughna S and Sato TN**. Antiopietin and Tie signalling pathways in vascular development. *Matrix Biol* 20: 319-25, 2001
- Majeti R**, Park CY, Weissman IL. Identification of a hierarchy of multipotent hematopoietic progenitors in human cord blood. *Cell Stem Cell* 1(6): 635-45, 2007
- Man AJ**, Davis HE, Itoh A, Leach JK, and Bannerman P. Neurite outgrowth in fibrin gels is regulated by substrate stiffness. *Tissue Eng Part A* 17 (23-24): 2931-42, 2011
- Mizrak D.**, Brittan M., Alison M.R. CD133: Molecule of the moment. *J Pathol* 214 (1): 3–9, 2008
- Mund JA, and Case J**. The role of circulating endothelial progenitor cells in tumor angiogenesis. *Curr Stem Cell Res Ther* 6(2): 115-21, 2011
- Muschler GF**, Nakamoto C and Griffith LG. Engineering principles of clinical cell-based tissue engineering. *J Bone Joint Surg Am* 86: 1541, 2004

- Nehls V**, Schuchardt E, Drenckhahn D. The effect of fibroblasts, vascular smooth muscle cells, and pericytes on sprout formation of endothelial cells in a fibrin gel angiogenesis system. *Microvasc Res* 48(3): 349-63, 1994
- Nielsen JS**, and McNagny KM. Novel functions of the CD34 family. *J of Cell Science* 121(22): 3682-92, 2008
- Nillesen STM**, Geutjesa PJ, Wismansa R, Schalkwijkb J, Daamena WF, and van Kuppevelta TH. Increased angiogenesis and blood vessel maturation in acellular collagen-eparin scaffolds containing both FGF2 and VEGF. *Biomaterials* 28: 1131, 2007
- Nixon AJ**, Watts AE, and Schnabel LV. Cell- and gene-based approaches to tendon regeneration. *J Shoulder Elbow Surg* 2: 278-94, 2012
- Noguera-Troise I**, Daly C, Papadopoulos NJ, Coetzee S, Boland P, Gale NW, Lin HC, Yancopoulos GD, and Thurston G. Blockade of Dll4 inhibits tumour growth by promoting non-productive angiogenesis. *Nature* 444: 1032-7, 2006
- Ott HC**, Matthiesen TM, Goh SK, Black LD, Kren SM, Netoff TI, and Taylor DA. Perfusion-decellularized matrix: using nature's platform to engineer a bioartificial heart. *Nat Med* 14: 213, 2008
- Perets A**, Baruch Y, Weisbuch F, Shoshany G, Neufeld G, and Cohen S. Enhancing the vascularization of threedimensional porous alginate scaffolds by incorporating controlled release basic fibroblast growth factor microspheres. *J Biomed Mater Res A* 65A: 489, 2003
- Pavelka M and Roth J**. Functional Ultrastructure: An Atlas of Tissue Biology and Pathology. *Springer*. p. 232, 2005
- Pedroso DC**, Tellechea A, Moura L, Fidalgo-Carvalho I, Duarte J, Carvalho E, and Ferreira L. Improved survival, vascular differentiation and wound healing potential of stem cells co-cultured with endothelial cells. *PLoS* 6 (1): e16114, 2011
- Pepper MS**. Transforming growth factor- β : vasculogenesis, angiogenesis, and vessel wall integrity. *Cytokine Growth Factor Rev* 8: 21-43, 1997
- Ribatti D**, Gualandris A, Bastaki M, Vacca A, Iurlaro M, Roncali L, and Presta M. New model for the study of angiogenesis and antiangiogenesis in the chick embryo chorioallantoic membrane. The gelatin sponge chorioallantoic membrane assay. *J Vasc Res* 34: 455, 1997
- Richardson TP**, Peters MC, Ennett AB, and Mooney DJ. Polymeric system for dual growth factor delivery. *Nat Biotechnol* 19: 1029, 2001
- Risau W and Flamme I**. Vasculogenesis. *Ann Rev Cell Dev Biol* 11: 73, 1995
- Sanai N**, Alvarez-Buylla A, and Berger MS. Neural stem cells and the origin of gliomas. *N Engl J Med*, 353 (8): 811-22, 2005
- Sartore S**, Chiavegato A, Faggin E, Franch R, Puato M, Ausoni S, and Pauletto P. Contribution of adventitial fibroblasts to neointima formation and vascular remodeling: from innocent bystander to active participant. *Circ Res* 89: 1111-21, 2001
- Schächinger V**, Assmus B, Britten MB, Honold J, Lehmann R, Teupe C, Abolmaali ND, Vogl TJ, Hofmann WK, Martin H, Dimmel S, Zeiher AM. Transplantation of progenitor cells and regeneration enhancement in acute myocardial infarction: final one-year results of the TOPCARE-AMI Trial. *J Am Coll Cardiol* 44 (8): 1690-9, 2004
- Singh SK**, Clarke ID, Terasaki M, Bonn VE, Hawkins C, Squire J, and Dirks PB. Identification of a cancer stem cell in human brain tumors. *Cancer Res* 63 (1): 5821-8, 2003
- Shmelkov S**, St Clair R, Lyden D, and Rafii S. AC133/CD133/Prominin-1. *Int J Biochem Cell Biol* 37 (4): 715-9, 2005
- Smith JD**, Chen A, Ernst LA, Waggoner AS, and Campbell PG. Immobilization of aprotinin to fibrinogen as a novel method for controlling degradation of fibrin gels. *Bioconjug Chem* 18(3): 695-701, 2007
- Suchting S**, Freitas C, le Noble F, Benedito R, Breant C, Duarte A, and Eichmann A. The Notch ligand Delta-like 4 negatively regulates endothelial tip cell formation and vessel branching. *Proc Natl Acad Sci USA* 104: 3225-30, 2007
- Sun Q**, Chen RR, Shen Y, Mooney DJ, Rajagopalan S, and Grossman PM. Sustained vascular endothelial growth factor delivery enhances angiogenesis and perfusion in Ischemic hind limb. *Pharm Res* 22: 1110, 2005
- Tomasek JJ**, Gabbiani G, Hinz B, Chaponnier C, and Brown RA. Myofibroblasts and mechano-regulation of connective tissue remodelling. *Nat Rev Mol Cell Biol* 3: 349-63, 2002
- van Hinsbergh VW, and Koolwijk P**. Endothelial sprouting and angiogenesis: matrix metalloproteinases in the lead. *Cardiovasc Res* 78: 203-12, 2008

- Verseijden** F, Posthumus-van Sluijs SJ, van Neck JW, Hofer SO, Hovius SE, van Osch GJ. Vascularization of prevascularized and non-prevascularized fibrin-based human adipose tissue constructs after implantation in nude mice. *J Tissue Eng Regen Med* 6 (3): 169-78, 2012
- Yana** I, Sagara H, Takaki S, Takatsu K, Nakamura K, Nakao K, Katsuki M, Taniguchi S, Aoki T, Sato H, Weiss SJ, and Seiki M. Crosstalk between neovessels and mural cells directs the site-specific expression of MT1-MMP to endothelial tip cells. *J Cell Sci* 120 (9): 1607–14, 2007
- Yancopoulos** GD, Davis S, Gale NW, Rudge JS, Wiegand SJ, and Holash J. Vascular-specific growth factors and blood vessel formation. *Nature* 407: 242-8, 2000
- Yang** S, Graham J, Kahn JW, Schwartz EA, and Gerritsen ME. Functional roles for PECAM-1 (CD31) and VE-cadherin (CD144) in tube assembly and lumen formation in three-dimensional collagen gels. *Am J Pathol* 155: 887, 1999
- Yang** HS, La WG, Cho YM, Shin W, Yeo GD, and Kim BS. Comparison between heparin-conjugated fibrin and collagen sponge as bone morphogenetic protein-2 carriers for bone regeneration. *Exp Mol Med* 44(5): 350-5, 2012
- Wang**, Y.H., Liu, Y., Maye, P., and Rowe, D.W. Examination of mineralized nodule formation in living osteoblastic cultures using fluorescent dyes. *Biotechnol Prog* 22: 1697, 2006
- Wolbank** S, Peterbauer A, Fahrner M, Hennerbichler S, van Griensven M, Stadler G, Redl H, and Gabriel C. Dose-dependent immunomodulatory effect of human stem cells from amniotic membrane: a comparison with human mesenchymal stem cells from adipose tissue. *Tissue Eng* 13: 1173-83, 2007
- Zengin** E, Chalajour F, Gehling UM, Ito WD, Treede H, Lauke H, Weil J, Reichenspurner H, Kilic N, and Ergün S. Vascular wall resident progenitor cells: a source for postnatal vasculogenesis. *Development* 133(8): 1543-51, 2006
- Zhang** HZ, Hayashi T, Tsuru K, Deguchi K, Nagahara M, Hayakawa S, Nagai M, Kamiya T, Osaka A, and Abe K. Vascular endothelial growth factor promotes brain tissue regeneration with a novel biomaterial polydimethylsiloxanetetraethoxysilane. *Brain Res* 1132: 29, 2007

Thank you!

It is a pleasure to acknowledge the inestimable help I have received from my supervisor Dr. Wolfgang Holnthoner. He was a leading and friendly advisor and always provided technical support, constant patience during the study and writing the thesis.

I wish also to thank Univ. Prof. Dr. Heinz Redl, head of Ludwig Boltzmann Institute for clinical and experimental Traumatology for bringing in numerous good ideas and still giving me the freedom of conducting my work individually. Thanks also to Mrs Monika Grossauer for directing me through the system of the LBI as well as Susi for her help in obtaining necessary literature. I want to express my gratitude to my colleagues in Linz who constantly provided adipose derived stem cells and also to my colleague Alexandra Meisl, for her fast, flexible and still accurate histologic preparations. Without them, this thesis would include a fractional amount of the results shown!

Especially, I deeply thank my parents for their moral support and to my siblings Marina, Horst and Peter for their refreshing presence. Thanks also to my friends and colleagues, who helped me in many different ways. Finally, thanks a lot to my boyfriend Martin Höbart, who always had a sympathetic ear for my thoughts and worries and who provided a calm and stable environment during the phase of writing.